

中華民國獸醫病理學會第411次組織病理會議
Chinese Society for Veterinary Pathology
411th Histopathology Seminar

人工智慧於數位毒性病理學之應用
(The application of artificial Intelligence in
digital toxicologic pathology)

廖俊旺

Jiunn-Wang Liao D.V.M., Ph. D.

中興大學獸醫學院獸醫病理生物學研究所
Graduate Institute of Veterinary Pathobiology
National Chung Hsing University

Date : May 16, 2025

課程大綱

1. 病理學**三次演化過程**
2. 人工智慧於數位毒性病理學應用之**經驗分享**
3. 利用人工智慧應用於毒性病理學之**國內外趨勢**
4. 總結及問題與**討論**

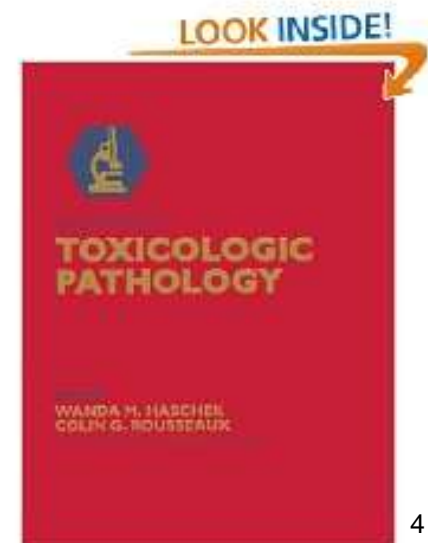
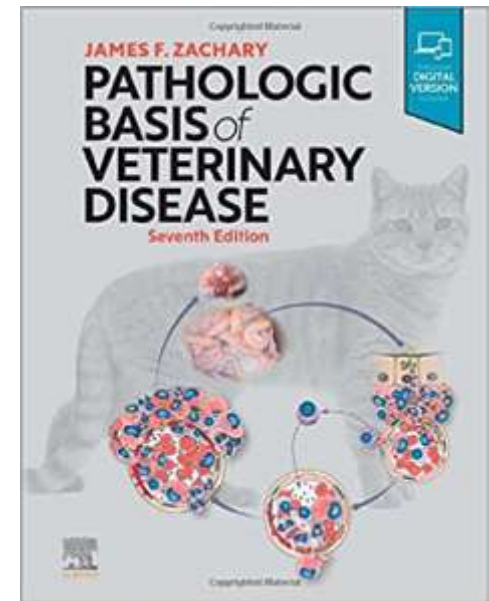


The Goals of Veterinary Pathology

1. **Veterinary pathology** is a medical specialty that studies the lesions and mechanisms of diseases affecting animal species.
 - 1.1. In **diagnostic pathology** an **autopsy** (synonym: **necropsy**) may be performed to (1) determine **the cause of death** of an individual animal or multiple animals in a herd, flock, kennel, or cattery
 - 1.2. **Surgical pathology** involves sampling a tissue **by biopsy** or fine needle aspirate (i.e., **cytology**) and using the information acquired from evaluating the specimen to establish a diagnosis, prognosis, and therapy **for the living animal**
 - 1.3. In **forensic pathology** the purpose of an autopsy is to determine the **nature of death** from a legal perspective
 - 1.4. **Experimental pathology** occurs in research settings where the **pathologist designs laboratory studies** with the goal of correlating morphologic lesions with clinical, functional, genetic, immunologic, and/or biochemical information to **elucidate the pathogenesises of diseases**

Introduction

1. In animal diagnostics, the pathologist takes in investigating the causes of diseases of individual patients and groups of animals and in determining their zoonotic or epidemic potential
2. In the chemical and pharmaceutical industries, veterinary pathologists help ensure the safety of medicines, chemicals, and materials used in our daily lives

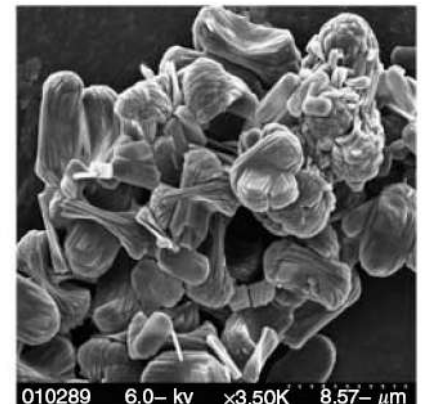
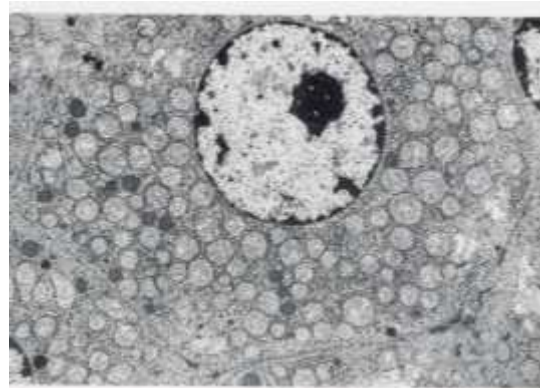
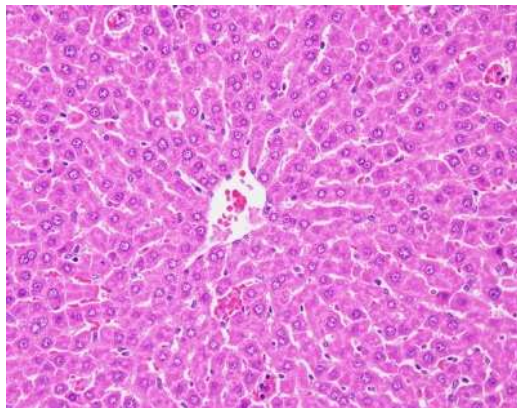


Instruments

Microscopy



SEM & TEM



Rat liver, H&E stain

Rat hepatocyte, TEM

Calcium oxalate, SEM

Morphologic diagnosis Differential diagnosis

Histopathological nomenclatures: (TDDDEM) Possible etiology

Tissue: Pneumonia, Hepatitis, Nephritis, Enteritis,

Distribution: Focal, Locally Extensive, Multifocal, Extensive and Diffuse, ...

Degree: Minimal, Slight, Moderate, Moderate/Severe, and Severe/High, ...

Duration: Acute, Subacute, and Chronic,

Exudate: Serous, Fibrinous, and Purulent,

Modifier: Necrotizing, Bronchointerstitial, Hemorrhagic, ...



Table 3-6 The Nomenclature of a Morphologic Diagnosis

Degree	Duration	Distribution	Exudate	Modifier	Tissue
Minimal	Acute	Focal	Serous	Necrotizing	Nephritis
Mild	Subacute	Multifocal	Catarrhal	Bronchointerstitial	Cystitis
Moderate	Chronic	Locally extensive	Fibrinous	Hemorrhagic	Enteritis
Marked (severe)	Chronic-active	Diffuse (interstitial) Cranoventral [†]	Suppurative Granulomatous	Embolic	Pneumonia* Hepatitis

This table provides an example of how nomenclature can be used to construct a morphologic diagnosis. It is not intended to be all inclusive and may vary from schemes used in other veterinary colleges.

*In the lung, it is customary to use the term pneumonia to indicate inflammation of the lung.

[†]Used only for diseases of the lungs.

Toxicologic pathology

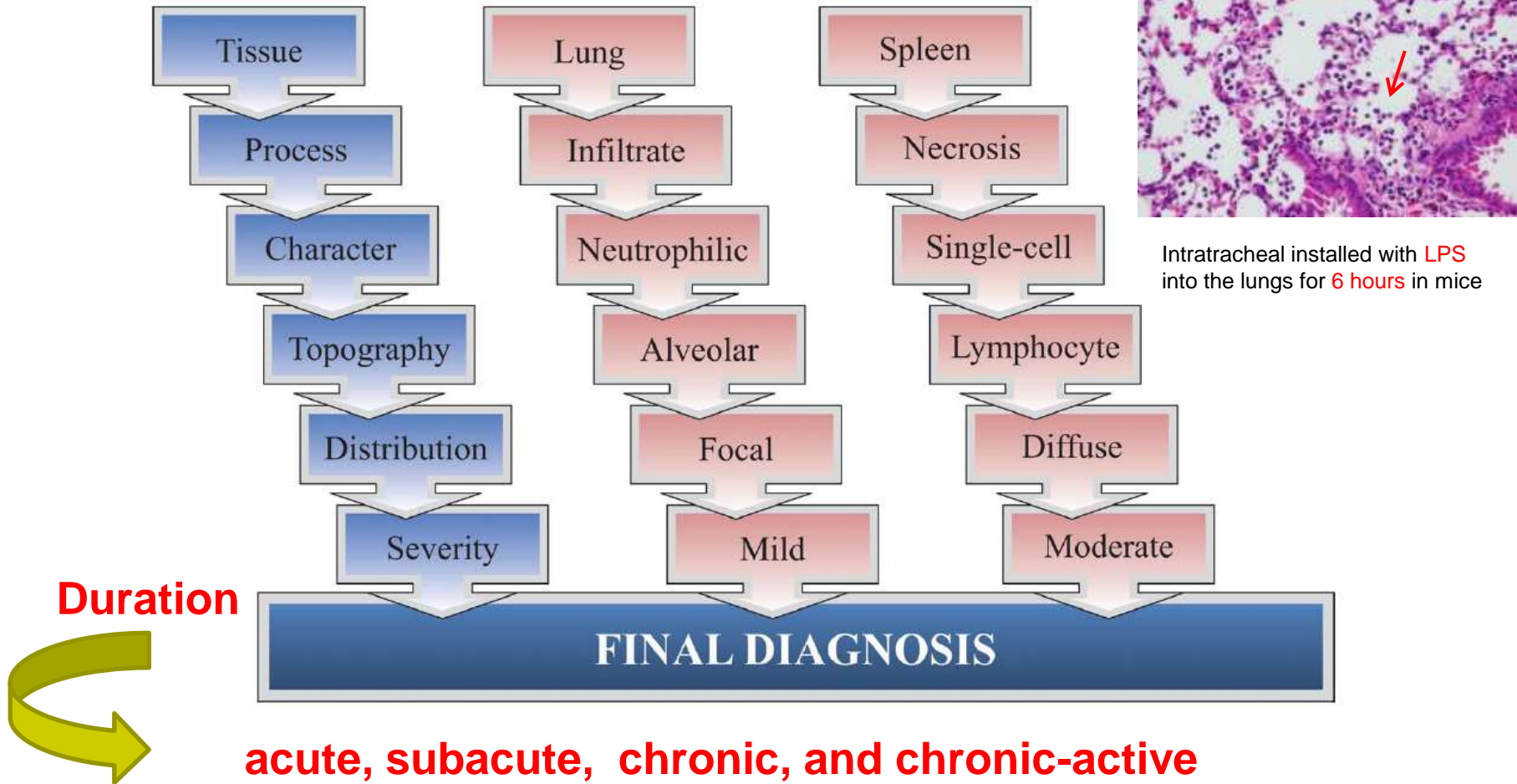
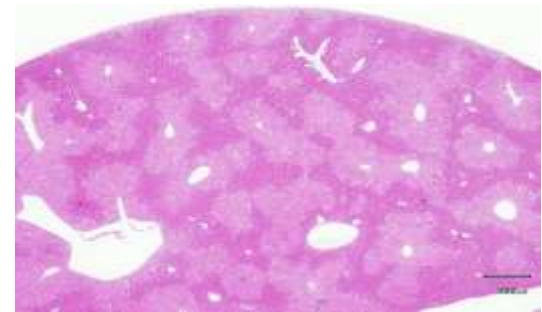


FIGURE 2.—Organization of a final diagnosis. Various modifiers and severity grades can be added to a basic key term or diagnosis to describe and categorize microscopic observations. In blue is an example of the fields possible in a diagnostic term, and examples are in red

Toxicologic pathology

- Toxicologic pathology is the study of the molecular, cellular, tissue, organ, and organism-level **response to novel agents**
- Three primary quality indicators of recording observations in **toxicologic pathology reports** have been identified:
 1. **Thoroughness**
 2. **Accuracy**
 3. **Consistency**
- The significance of **non-neoplastic lesions** can be recorded either **semiquantitatively** by applying defined **severity grades** or **quantitatively** by using **image analysis** and stereological techniques to provide numerical values for specific lesions



CCl₄-induced acute coagulated necrosis, mouse

Grading scheme I

- 0 = Not present
- 1 = Minimal (<1%)
- 2 = Slight (1–25%)
- 3 = Moderate (26–50%)
- 4 = Moderately Severe/high (51–75%)
- 5 = Severe/high (76–100%)

The revolution in pathology

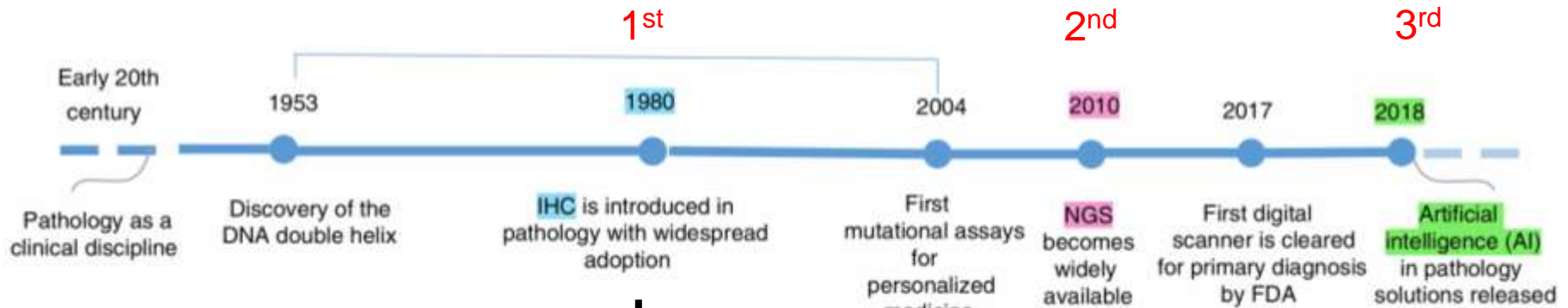
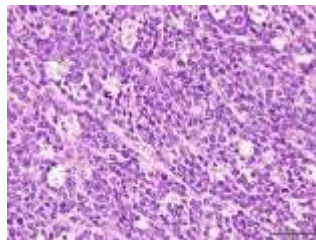


Figure 1. Chronology of the 'three revolutions' in pathology.

Manuel Salto-Tellez.
Histopathology
2019, 74, 372–376.



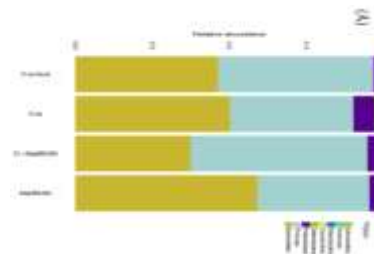
Hematoxylin and eosin (H&E)



CD4 (+++)

Pre-T LBL, thymic lymphoma in NOD/SCID mice

Next Generation Sequencing (NGS)-based microbiota analyses



AI-based approaches, whole-slide imaging (WSI)



(DotSlide, Olympus, Germany)

FIND AN EXPERT

Professor Manuel **Salto Tellez**
Chair of Molecular Pathology at **Queen's University** Belfast, UK
Director of Queen University Belfast's **Precision Medicine Centre of Excellence**, Consultant Histopathologist and Molecular Diagnostician.

Precision Medicine Centre of Excellence

Professor Salto Tellez is an international pathologist and is one of the drivers behind the Precision Medicine Centre of Excellence.

“Who would have predicted years ago that molecular diagnostics, precision medicine, cancer immunotherapy and **artificial intelligence would redefine the future of modern pathology?**” says Professor Salto Tellez. His advocacy and work on digital pathology and morpho-molecular diagnostics across Europe, the UK and USA has helped the future of modern pathology.

Professor Salto Tellez is a leading academic medical practitioner in his area of expertise. He has been part of international working groups advising the US NIH and other national and international institutions. One of his latest research programmes is a Cancer Research UK Accelerator Award to foster the use of artificial intelligence and digital pathology in cancer research and cancer diagnostics. Professor Salto Tellez believes in a true synergy between healthcare, academia and industry.

FIELDS



CONTACT INFORMATION

For more information or to book an interview, email comms.office@qub.ac.uk

[ACADEMIC PROFILE >](#)

RELATED EXPERTS

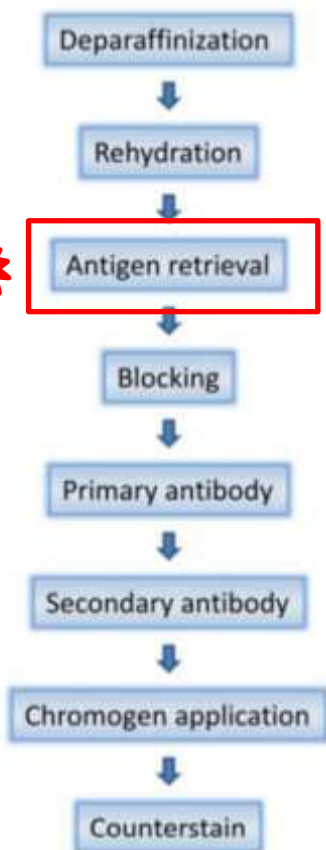
- [Dr Amy Jayne McKnight](#)
- [Dr Ciaran Mulholland](#)
- [Dr Connor Bamford](#)

The 1st revolution: Immunohistochemistry (IHC)

1. **IHC**, became a regular component of the pathologist's diagnostic armamentarium during the **late 1980s and early 1990s**.
2. **IHC** involved the **same** qualitative visual interpretation and subjectivity **as histology**.
3. Evaluation of the **intensity of the expression of the proteins**, the **subcellular localisation** and the **tissue types** expressing them provided important information regarding both **diagnosis and discovery**.
-  4. This almost universal availability (**‘the best thing about IHC is that everyone can do it’**), however, has not come without criticism (**‘the worst thing about IHC is that everyone can do it’**), perhaps highlighting the need for more rigorous design, validation and delivery of IHC.
5. The adoption of IHC became the first main substantial change in the practice of **diagnostic pathology: a true revolution**

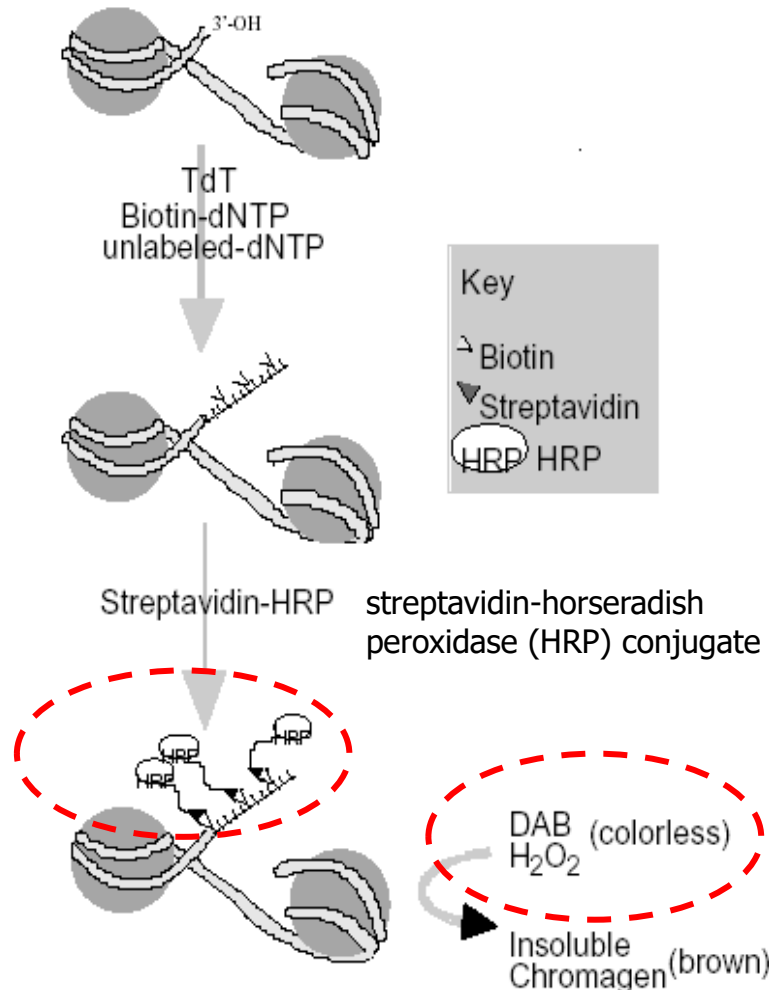
Immunohistochemistry method

DNA FRAGMENTATION DETECTION KIT

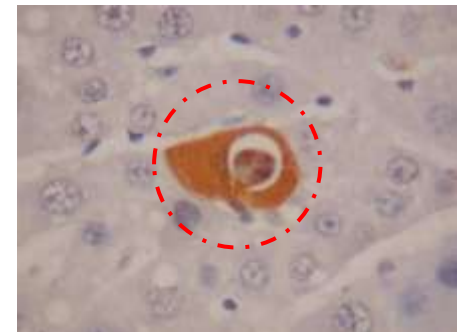


Methods Mol Biol. 2019 ;
1897: 289–298

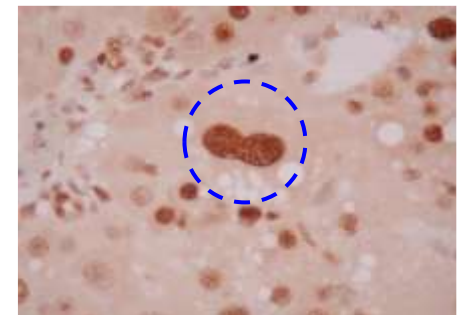
Nucleosomal DNA Fragment



Oncogene Research Products
QIA33 TdT-FragELTM, 2001



Apoptosis, IHC



PCNA, IHC, Overstaining

Differential diagnosis

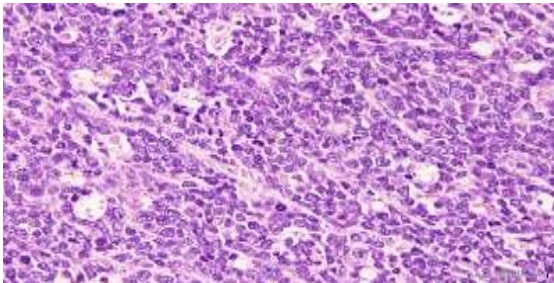
Cho-Yen Tsai (蔡卓諺), 394th CSVP, 2023



NOD.CB17-Prkdcscid/JTcu
(NOD/SCID) mice



A **thoracic mass** compressing heart and lung with pleural effusion



The neoplastic cells are **round to polygonal**, with abundant eosinophilic cytoplasm

Round cell tumor, Lymphoma? B or T?...

B-cell neoplasms

Precursor B-cell neoplasm

Precursor B-cell lymphoblastic lymphoma/leukemia (pre-B LBL)

Mature B-cell neoplasms

Small B-cell lymphoma (SBL)

Splenic marginal zone B-cell lymphoma (SMZL)

Follicular B-cell lymphoma (FBL)

Diffuse large B-cell lymphoma (DLBCL)

Morphologic variants

Centroblastic (CB)

Immunoblastic (IB)

Histiocyte associated (HA)

Subtypes

Primary mediastinal (thymic) diffuse large B-cell lymphoma (PM)

Classic Burkitt lymphoma (BL)

Burkittlike lymphoma (including mature B-cell lymphomas with lymphoblastic morphology) (BLL)

Plasma cell neoplasm

Plasmacytoma (PCT)

Extraosseous plasmacytoma (PCT-E)

Anaplastic plasmacytoma (PCT-A)

B-natural killer cell lymphoma (BNKL)

T-cell neoplasms

Precursor T-cell neoplasm

Precursor T-cell lymphoblastic lymphoma/leukemia (pre-T LBL)

Mature T-cell neoplasm

Small T-cell lymphoma (STL)

T-natural killer cell lymphoma (TNKL)

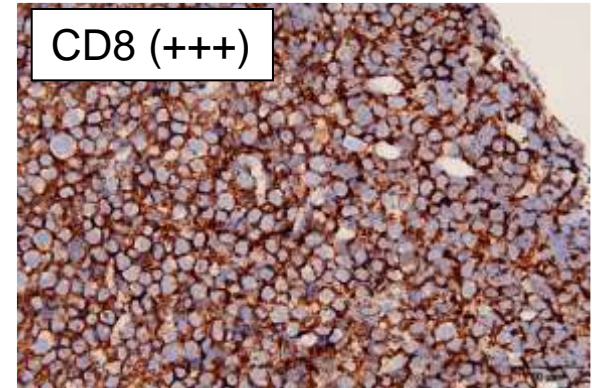
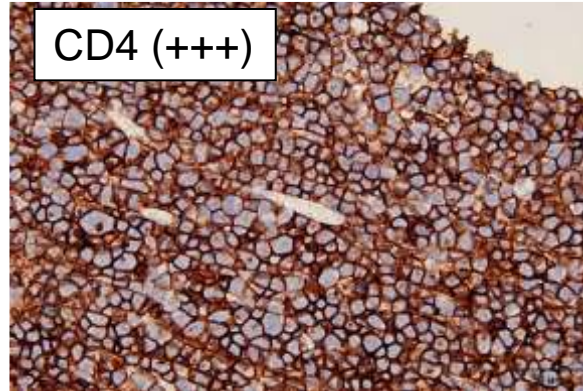
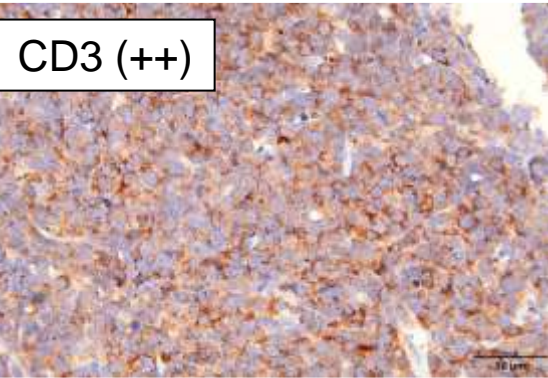
T-cell neoplasm, character undetermined

Large cell anaplastic lymphoma (TLCA)

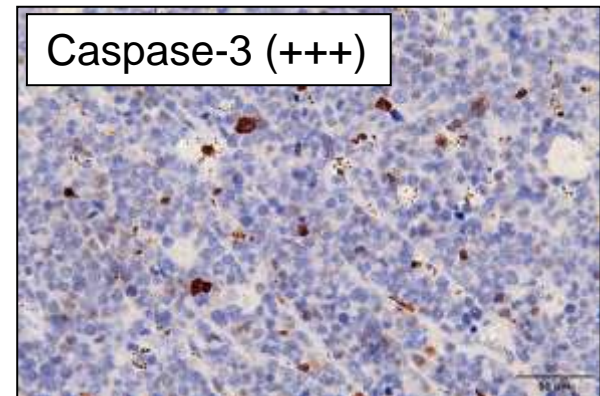
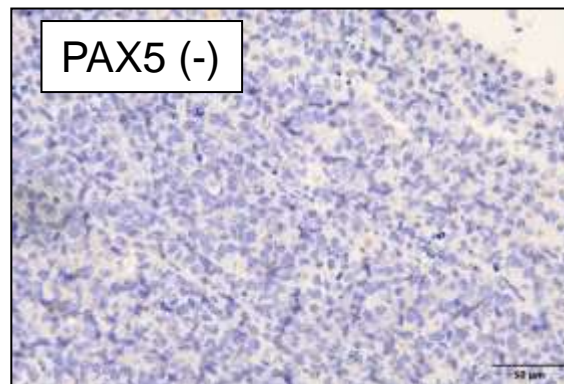
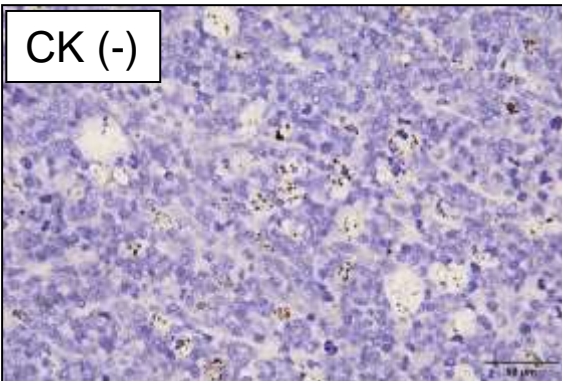
Pathological diagnosis: Precursor T-cell lymphoblastic lymphoma (Pre-T LBL, thymic lymphoma)

Marker	Target
CD3	T cell differentiation
CD4	Helper T cell
CD8	Cytotoxic T cell
CK	Epithelial differentiation
PAX5	B cell differentiation
Caspase-3	Apoptosis

T cell markers cluster of differentiation (CD)



B cell markers



The 2nd revolution: (the molecular diagnostic revolution)

1. **Molecular diagnostic** was only '**tangentially**' related to pure morphology during 2010. [tæŋ`dʒen[ə]l]切向的.
2. **Next-Generation Sequencing (NGS)** becomes widely available. However, the techniques, the concepts and the interpretation **did not require knowledge of the morphology of disease**, but rather of the molecular basis of disease.
3. The **controversy** as to who owns the **interpretation of the genomic information** in diagnostic/clinical practice has not abated.
4. Perhaps **pathologists are losing a great opportunity** by not embracing these technologies upfront and embedding **genomic medicine** as a element of tissue pathology training—so allowing pathologists to actively lead this second revolution, rather than simply facilitating

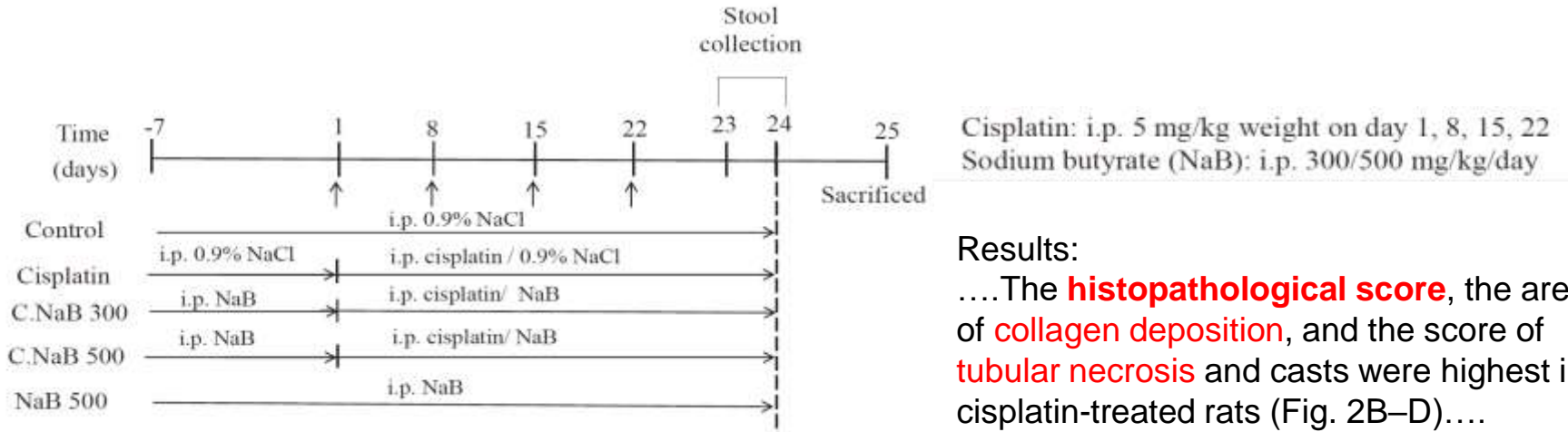


Technical Report

<https://www.hitachi-hightech.com/>

Butyrate modulates gut microbiota and anti-inflammatory response in attenuating cisplatin-induced kidney injury

W.-J. Chen et al. *Biomedicine&Pharmacotherapy* 181(2024)117689



Results:

....The **histopathological score**, the area of **collagen deposition**, and the score of **tubular necrosis** and casts were highest in cisplatin-treated rats (Fig. 2B–D)....

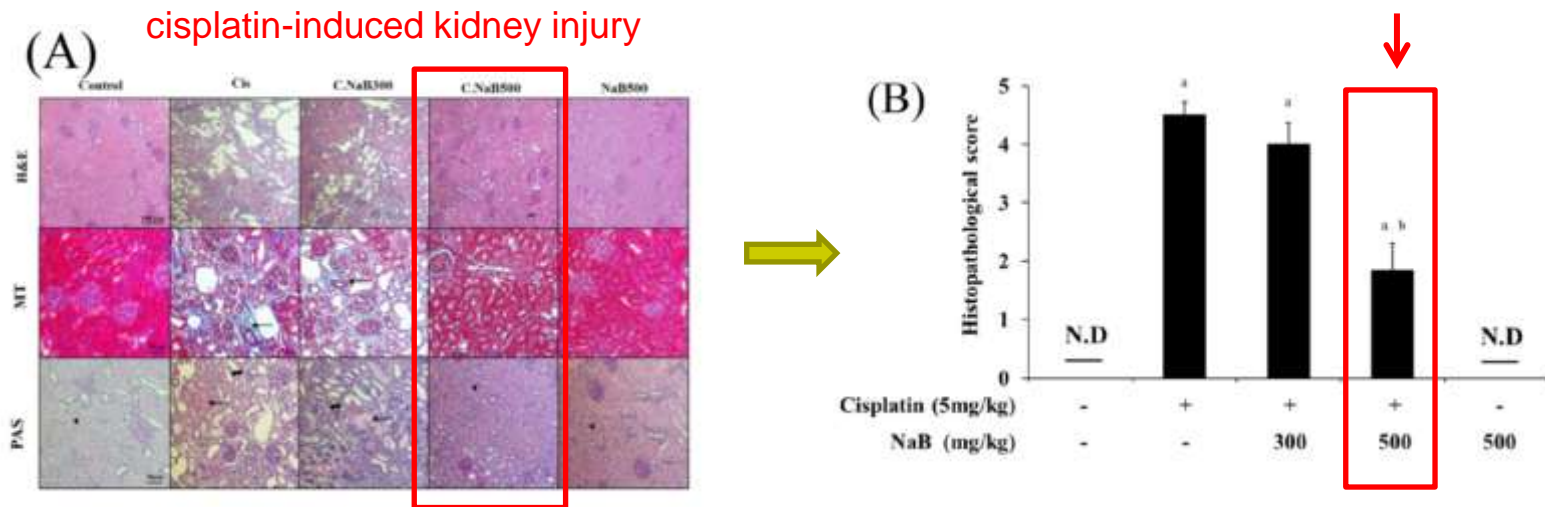


Fig. 2. Effect of butyrate treatment on changes in the histopathological examination of the kidney in cisplatin-treated rats. (A) Histopathological changes were examined by H&E staining, Masson's trichrome (MT) staining, and periodic acid-Schiff (PAS) staining. (B) The histopathological score of H&E staining.

4.7. Butyrate pretreatment effectively restores dysbiosis of intestinal microbiota in cisplatin rats by using **Next-Generation Sequencing (NGS)**-based microbiota analyses

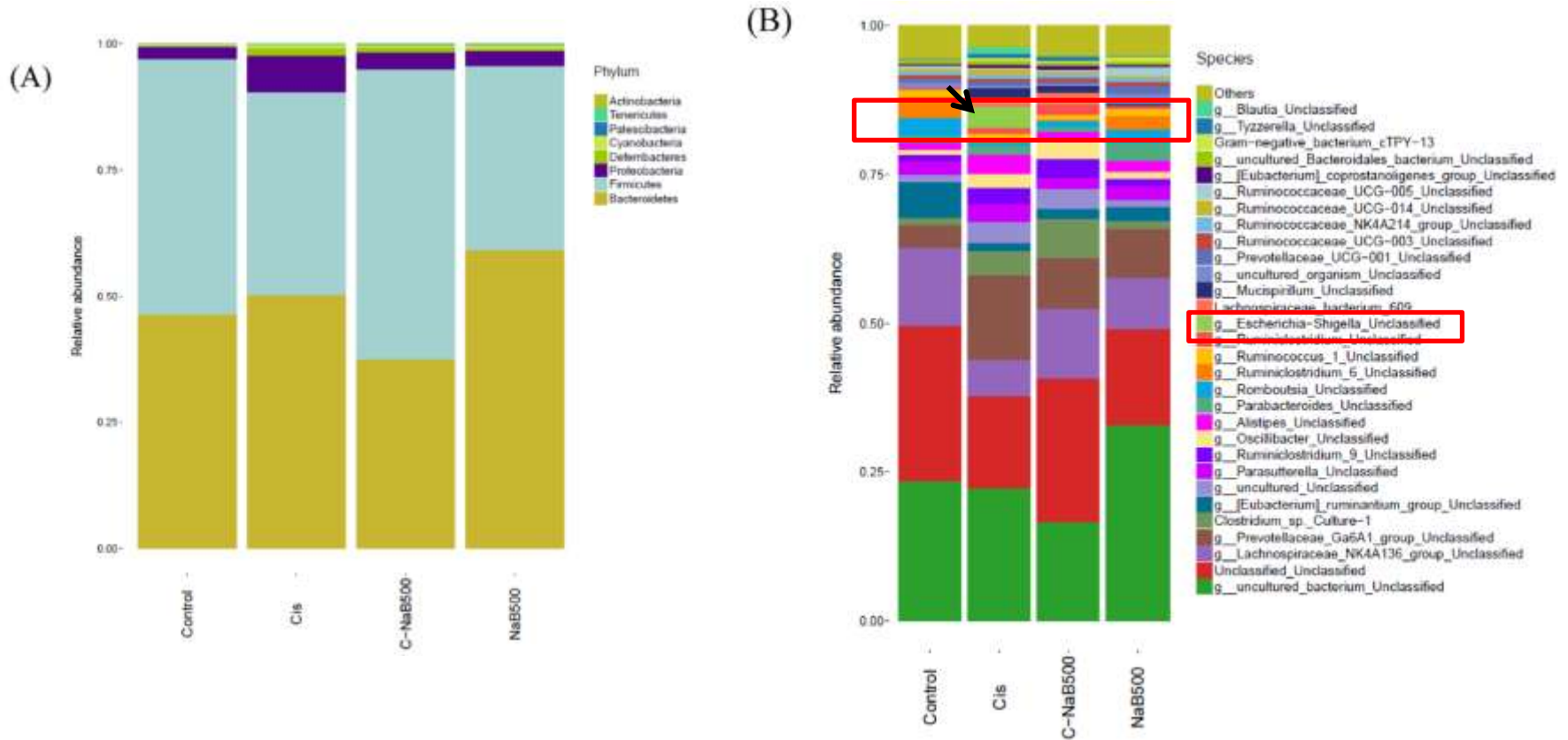
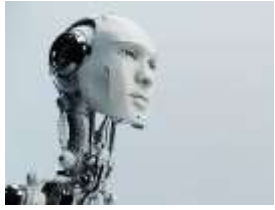


Fig. 7. Butyrate altered the gut microbiota composition in cisplatin-induced kidney rats.

...Specifically, we observed a decrease in the abundance of *Escherichia*, *Shigella* and *Blautia*, alongside an increase in the abundance of the butyrate producing genus *Roseburia*.



Artificial intelligence – the 3rd revolution in pathology

Humanoid robot

https://www.semi.org/zh/AIAgent_HumanoidRobot

1. The term “**artificial intelligence (AI)**” was initially introduced by John McCarthy at a 1956 Dartmouth conference on AI, defined then as “**the science and engineering of making intelligent machines.**”
Turner et al., Toxicologic Pathology 2020, Vol. 48(2) 277-294
2. AI represents an incipient third revolution that is **knocking loudly at the door of pathology**, with attendant opportunities and challenges
3. **AI** represents a range of **advanced machine technologies** that can derive meaning and understanding from extensive data inputs, in ways that **mimic human capabilities in**, for example, perceiving images
4. With **AI algorithms**, it is **becoming possible** to precisely and **automatically identify tissue** patterns that, for years, have been the exclusive domain of **pathologists** and the human **visual cortex**

Manuel Salto-Tellez. Histopathology 2019, 74, 372–376.

Machine technologies



1. imaging system for '**virtual microscopy**' the later being the digital equivalent to **conventional light microscopy**.
2. The single images initially acquired during the scanning process are automatically stitched together to form a large seamless overview image (the '**virtual slide**').
3. This digital virtual microscopy image can **be saved in a web-based database** and is accessible **for online conferencing, e.g. in pathology or histology**.

Multimedia e-learning environment

ScanScope® XT System, 2007



<http://www.vm.ntu.edu.tw/dplab/index.htm>

Dot slide, 2011



http://www.microscopy.olympus.eu/microscopes/Life_Science_Microscopes_dotSlide_-_Virtual_Slide_System.htm

Aperio, 2020



<http://140.120.114.107/slidecenter.php?id=545>

Digital pathology

- **Digital pathology** is a **dynamic, image-based** environment that enables the acquisition, management and interpretation of **pathology information** generated from a **digitized glass slide**.

<https://digitalpathologyassociation.org/about-digital-pathology>



<https://youtu.be/6fqVnoWnYxc>

病理切片 — SLIDE

登入切片系統



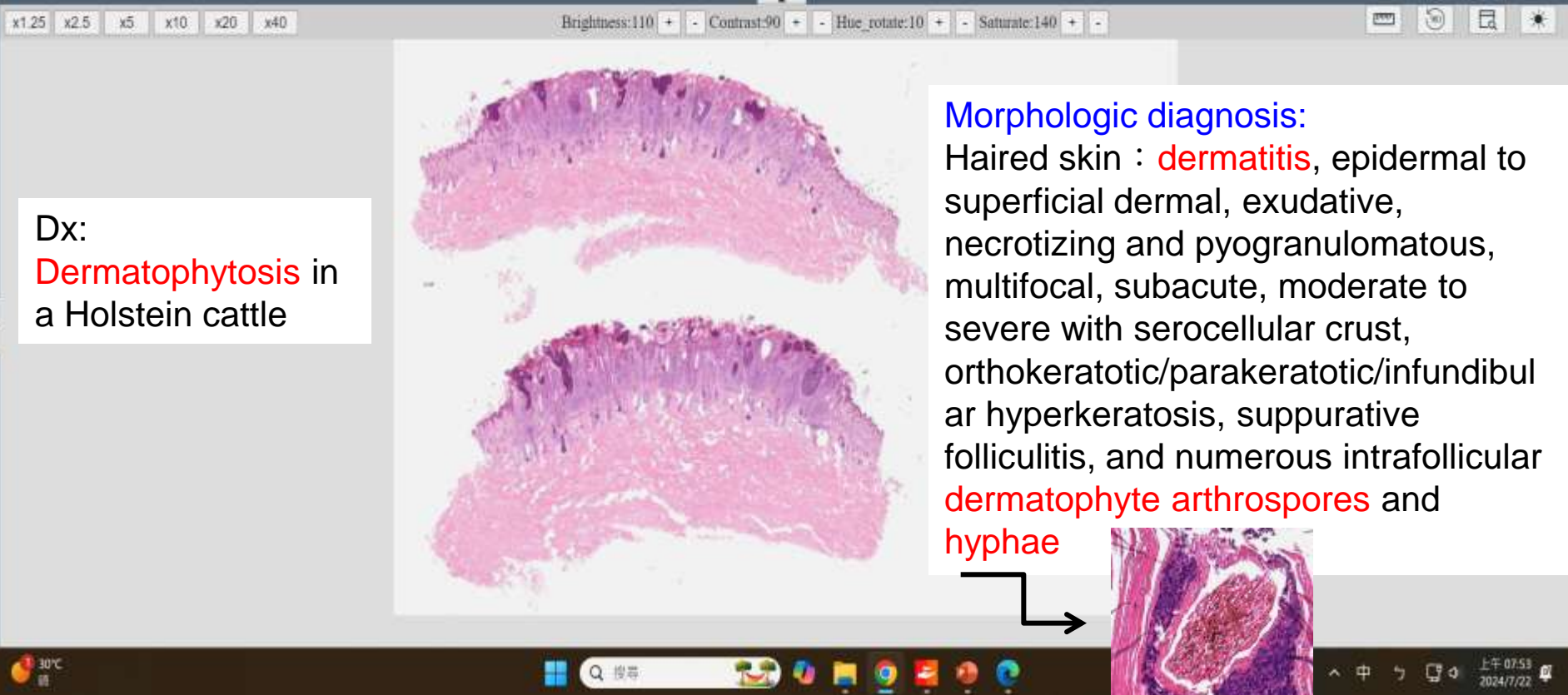
<http://140.120.114.107/slidecenter.php?id=545>



切片名稱 : Case 5. 2024-208-4

Case 5. CSVP 2024-3246 (2024-208-4, ADDC VRI, Y.W. Chen, Y.C. Chuang, S.C. Hu, F. Lee, and Y.C. Tu)

Holstein Cattle, adult, 2-year-old. The animal was stunted and culled by the owner. Abnormality in pre-slaughter examination was reported by the veterinarian. Multiple slightly-raised, white to gray skin nodules covered with crusted surfaces were noted, and mostly affected the head and upper body.



Dx:
Dermatophytosis in
a Holstein cattle

Morphologic diagnosis:
Haired skin : **dermatitis**, epidermal to superficial dermal, exudative, necrotizing and pyogranulomatous, multifocal, subacute, moderate to severe with serocellular crust, orthokeratotic/parakeratotic/infundibular hyperkeratosis, suppurative folliculitis, and numerous intrafollicular **dermatophyte arthrospores** and **hyphae**

The tissue diagnostic laboratory pathway

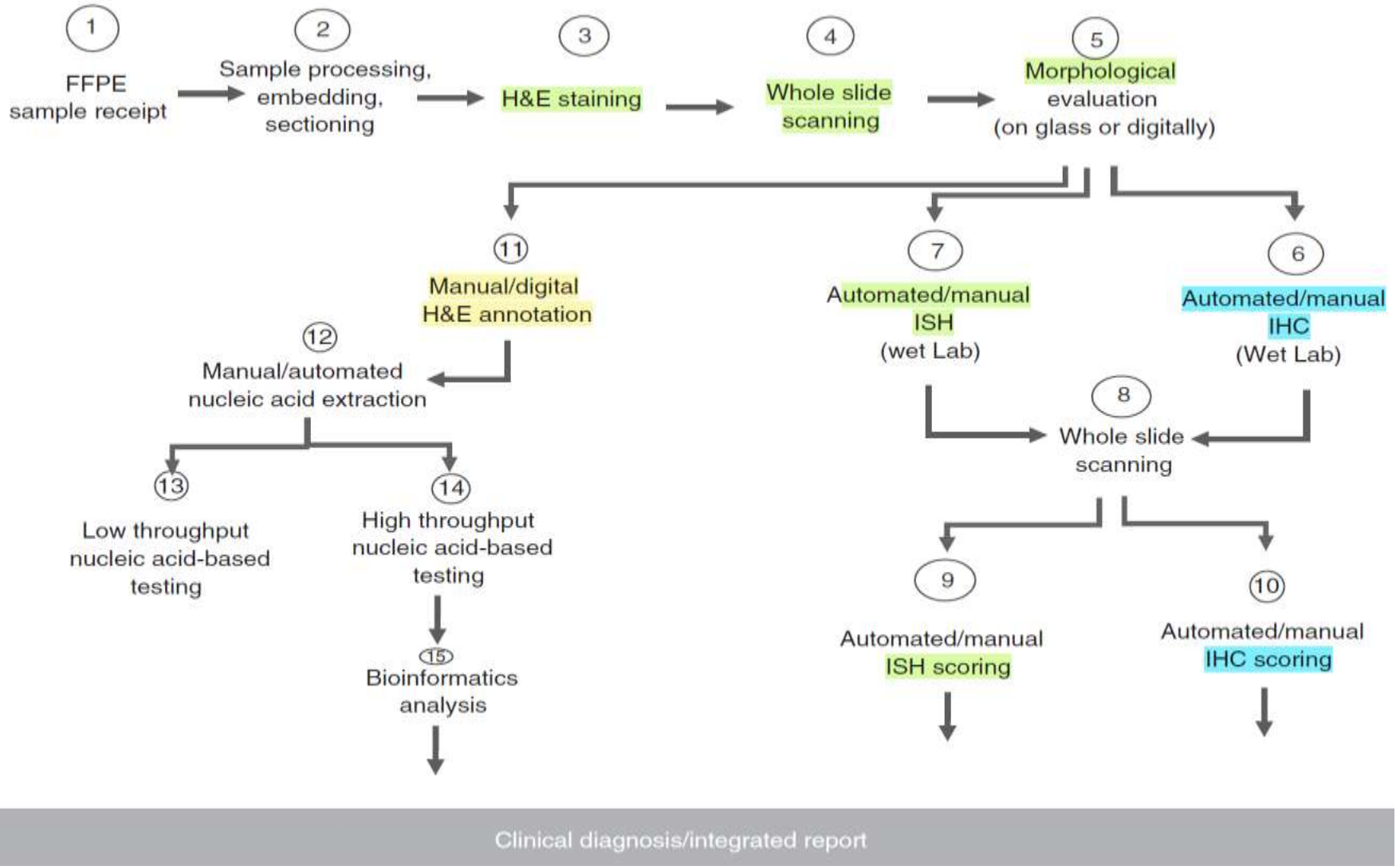


Figure 3. Steps in the tissue diagnostic pathway. FFPE, Formalin-fixed paraffin-embedded; H&E, Haematoxylin and eosin; IHC, Immunohistochemistry; ISH, In-situ hybridisation; NA, Nucleic acid.

Artificial intelligence (AI)

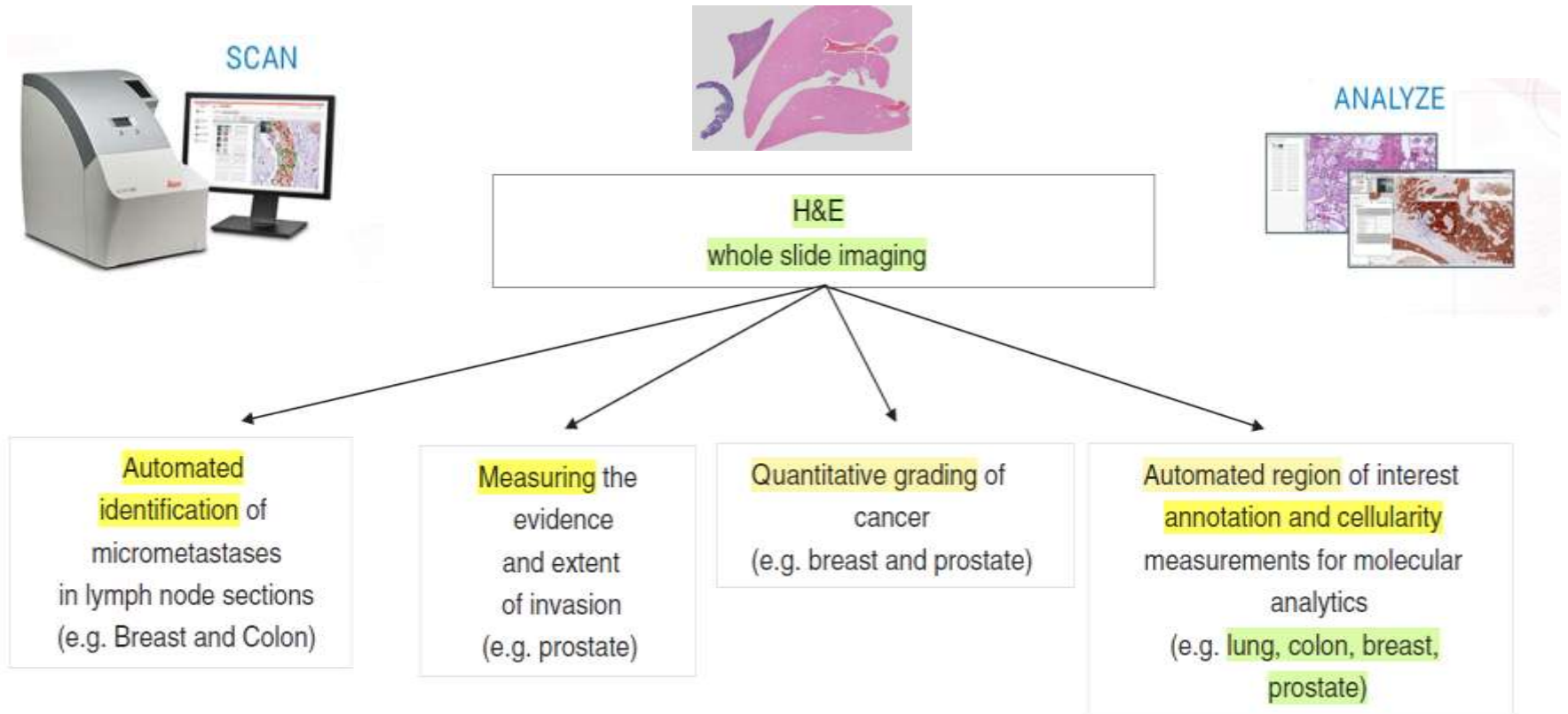
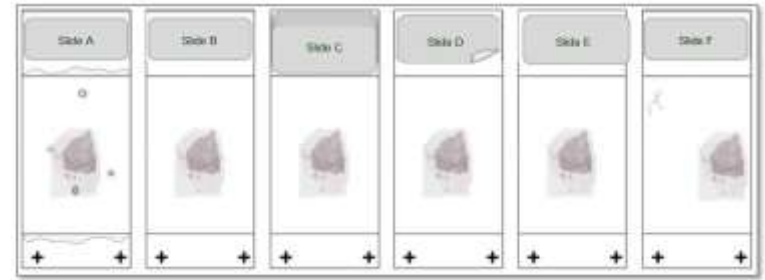


Figure 2. **How artificial intelligence (AI) may**, in the future, facilitate **multiple activities** related to the hematoxylin and eosin (H&E) sets of cases.

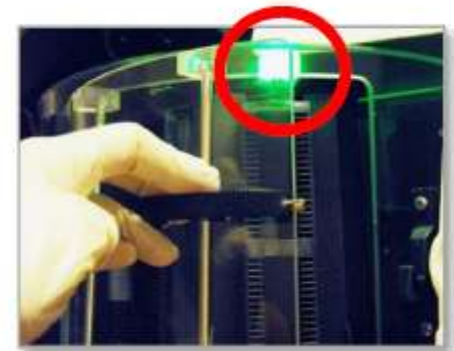
Digitization of glass slides



Autoloader



Slide Settings



Slide view

Scan

病理切片 — SLIDE

登入切片系統



Whole Slide Imaging

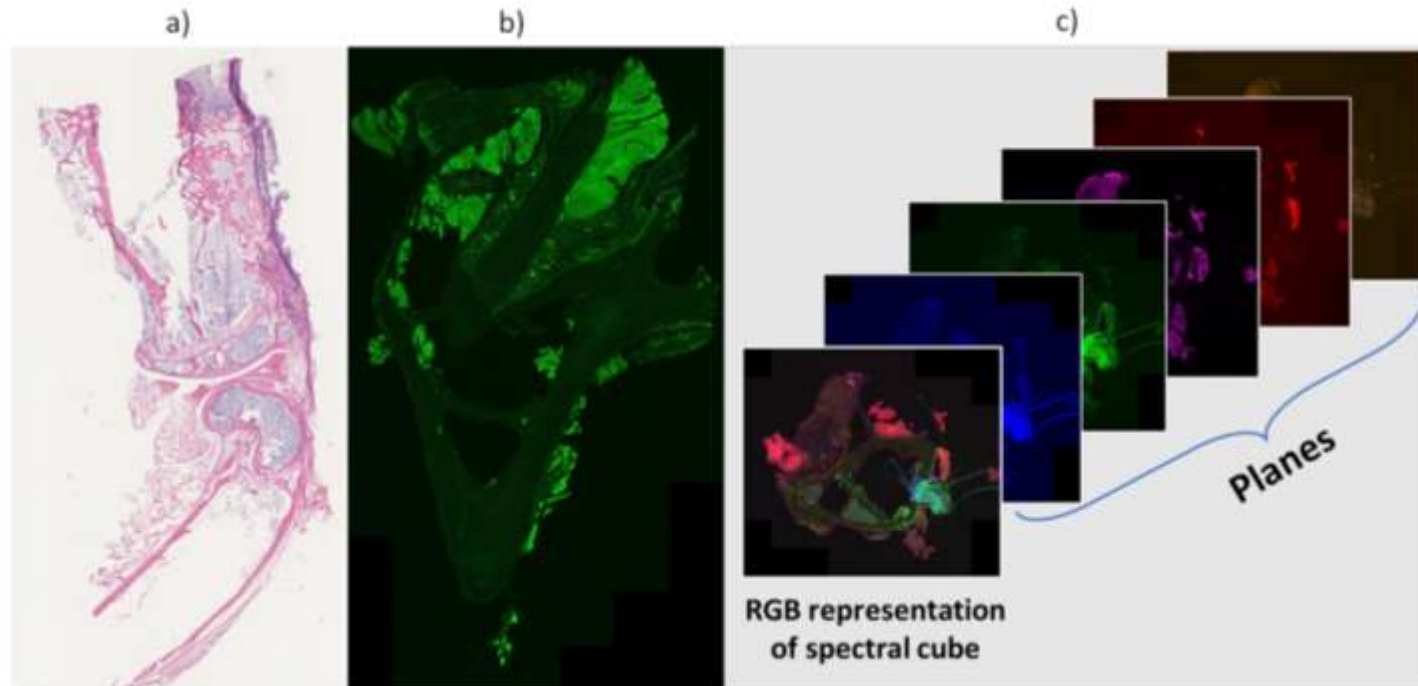


Fig. 1. Examples of WSI modalities.

(a) Bright field image, (b) Fluorescence image, and (c) Fluorescence multispectral, planes, and RGB representation cube. These images were provided by the Leibniz-Institut für Photonische Technologien, and correspond to different hard bone and bone marrow tissues of a mouse.

Pyramid image

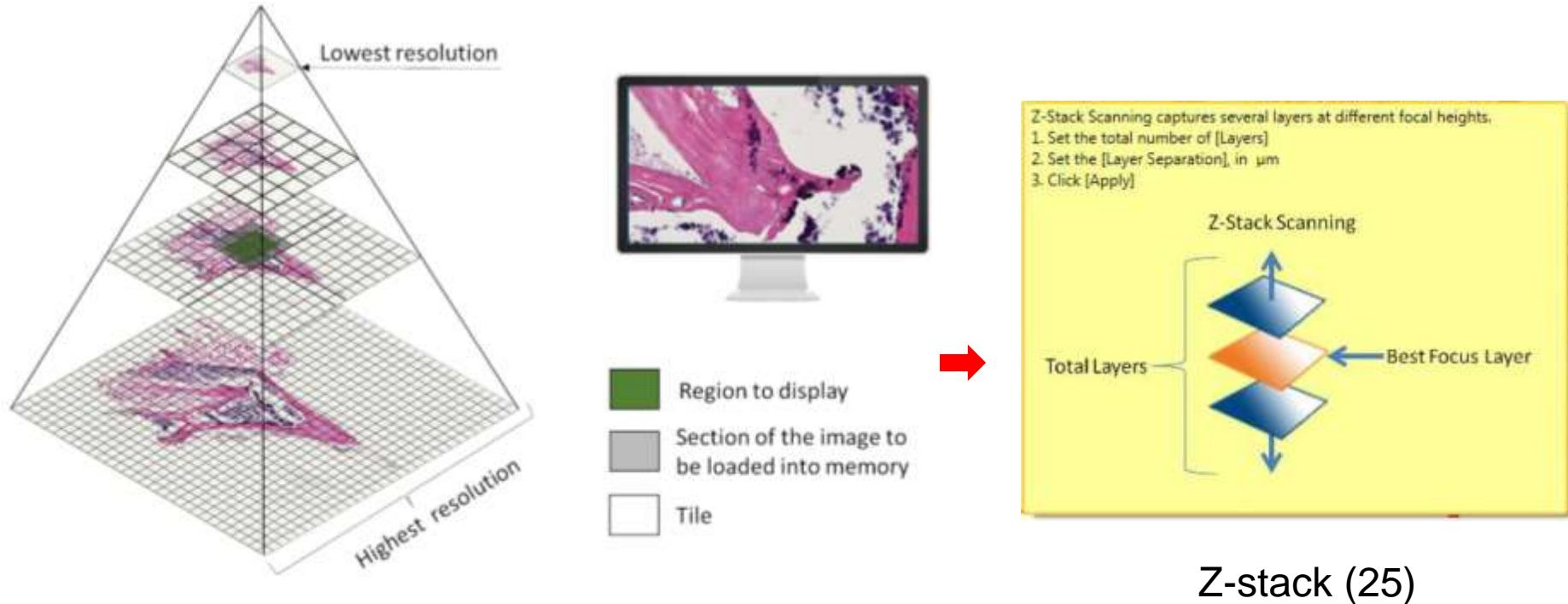


Fig. 2. Pyramid organization used to store and visualize WSIs.

This illustration shows a pyramid representation of a whole slide image with 4 levels. The top-level of the pyramid has the lowest resolution, the bottom level has the highest resolution, and the middle levels have intermediate resolutions. Each level is divided into two dimensional blocks called tiles (unfilled squares).

This image also shows the tiles that will be loaded in memory (Gray squares) to display a region of interest (Green squares). The resolution used (pyramid level) will depend on the zoom that is requested.

Image analysis

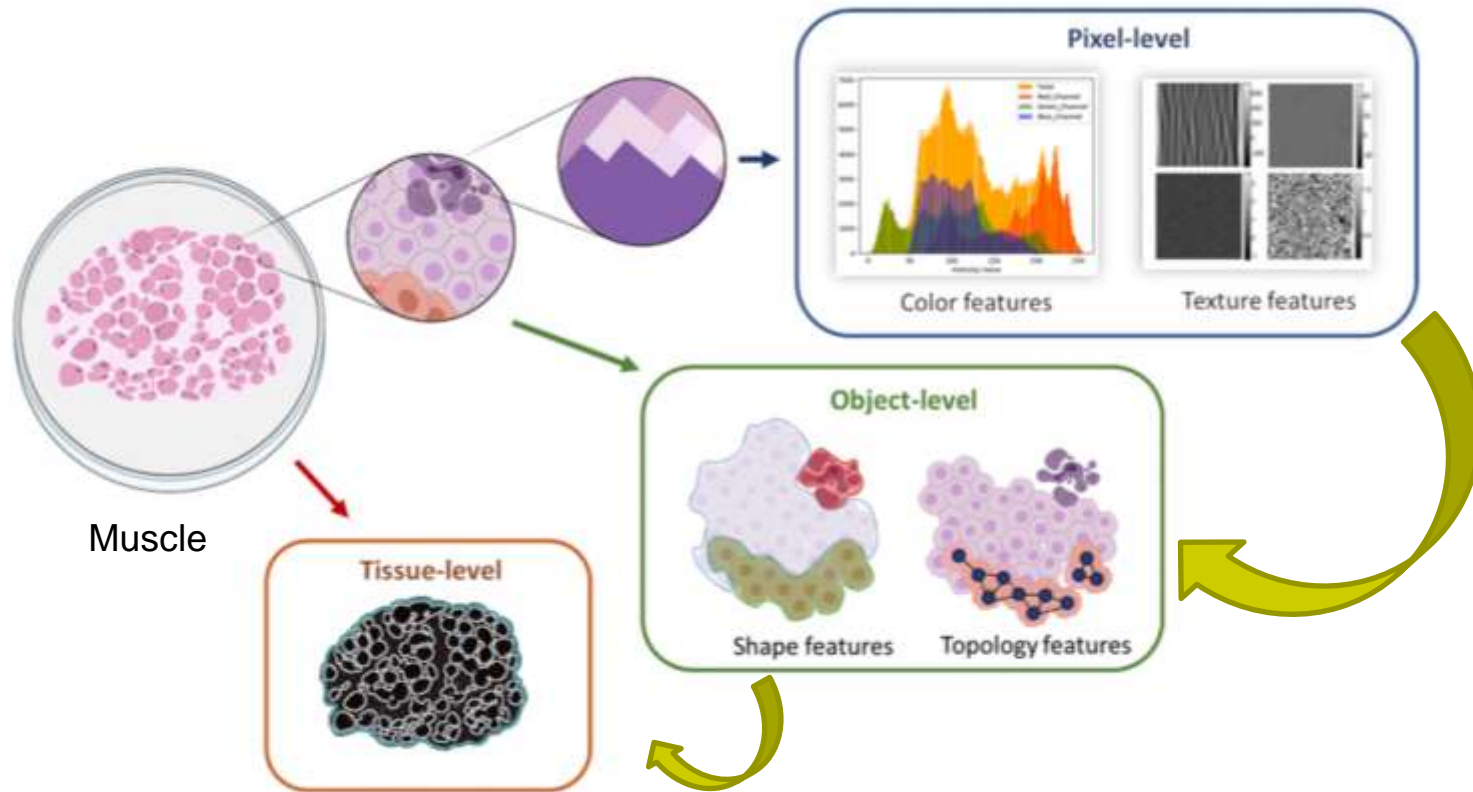


Fig. 3. Categorizing of image analysis levels according to magnification.

The identification and extraction of the features in the tissue are carried out at **different levels of magnification** (pixel, object, and tissue levels).

At the pixel-level, it is possible to analyze changes in intensity, edge discontinuities, frequency in the histogram, or saturation values.

At object-level, objects can be categorized by their morphological characteristics or by their topology.

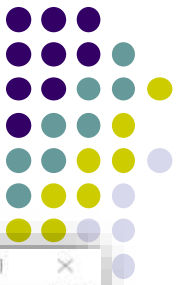
And at the tissue-level, the entire tissue structure is analyzed.

Table 2

Bio-imaging software used in DP comparison.

Tool	Way to work with WSIs	Main programming language	Machine learning tools	Main feature
ImageJ	Using SlideJ	Java	With plugins	It has a wide range of tools for image processing and has the largest community of users and developers Versatility, continuous improvements and ease of use by using pipelines process
CellProfiler	External software	Python	Yes	Cover a wide variety of biological applications and have cut edge algorithms
ICY	Using the plugin Icytomine or an external software	Java	With plugins	The segmentation, classification, tracking and counting of elements are its speciality
Ilastik	Using external software	Python	Yes	

ImageScope



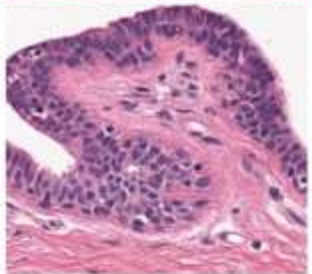
3. Annotations , 確認並匯出數據

The screenshot displays the Apero ImageScope v12.4.0.5043 interface. The main window shows a histology image with a cyan line tracing a boundary, and 25 yellow distance measurements labeled in micrometers (um). A 'Distance Measurement Tu...' dialog box is open, showing '# Measures' set to 25. The 'Annotations - Detailed View' window is open at the bottom, showing a table of measurement data. The table has columns for 'Region', 'Length (um)', and 'Area (um2)'. The first row is highlighted in blue, and the value '16.04' in the 'Length (um)' column is highlighted with a red box.

Region	Length (um)	Area (um2)
1	16.04	
2	26.07	
3	27.56	
4	24.44	
5	22.63	
6	24.41	
7	28.38	
8	29.46	
9	29.51	
10	31.02	
11	30.87	

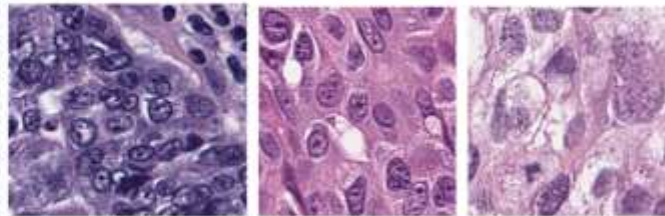
Challenges in the image analysis

1. Biological variation

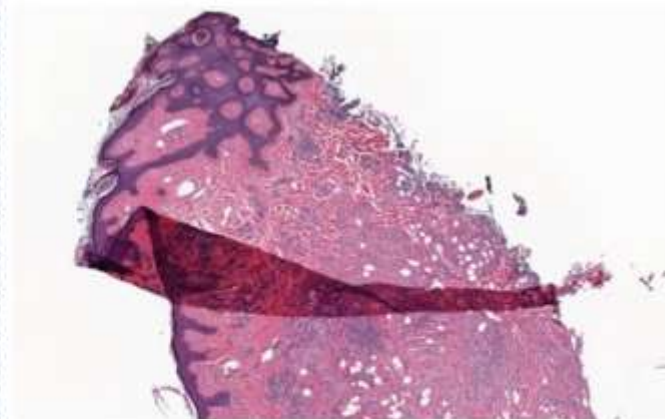


Breast tissue^α

2. Technological variation



Differences in staining processes^β

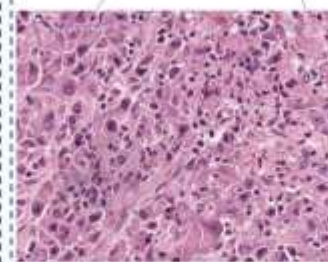


Folds in tissues^γ

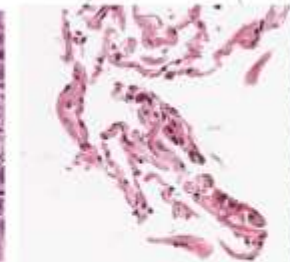
3. Pathological variation



Lung tissue^α



Anomaly

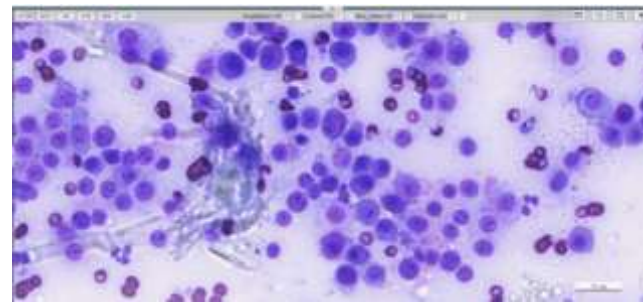
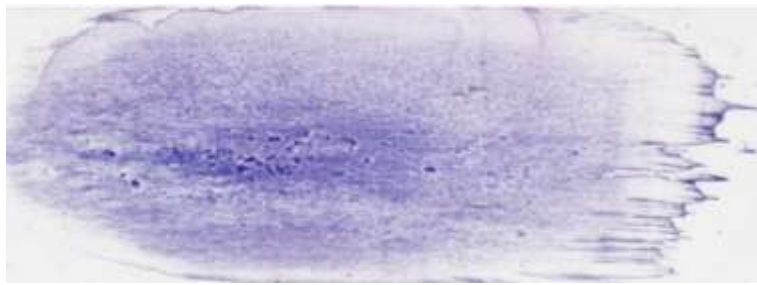


Normal

^α → PathPresenter repository. ^β → NuCLS dataset. ^γ → OpesSlide dataset.

Fig. 4. Examples of different types of variation in tissue images.

On the left of the image, different sections of the same tissue sample are shown, and one can see variations in the structure and the elements of the same sample. In the middle box, there are shown variations caused by **different staining techniques** using the **same type of tissue (breast)**. Moreover, a fold in the tissue which makes distortions in shape and color is shown. **On the right side, a tissue with healthy areas and areas with pathological alterations is shown.**



http://140.120.114.107/ivp_slide_view.php?id=2022

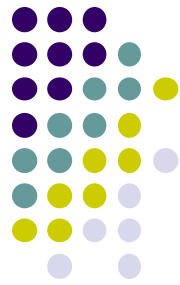


TABLE 1 Summary of advantages and disadvantages of whole slide imaging in cytopathology according to literature

	Advantages	Disadvantages
Area of interest		
The cytological specimen and the scanner	<ul style="list-style-type: none"> • High quality standardised slide⁴ • No more concern of slide breakage or fading of stains • Incentive to find workable technical solutions^{2,7} 	<ul style="list-style-type: none"> • Need of optimal slides before scanning⁴ • Need of Z-stack with multiple planes to reproduce focusing capability of LM¹⁰ • Longer scanning times • Greater file size • Potentially difficult electronic handling of image file²
The diagnosticians' work	<ul style="list-style-type: none"> • Unlimited annotations by different viewers¹² • Simultaneous viewing • Easy sharing of difficult cases • Possibility to work at distance • Possible side-by-side comparison of cases • Previous cases of the same patients available in the digital systems 	<ul style="list-style-type: none"> • Longer times to navigate slides • Potential latency or freezing of slides if not adequate informatics requirements • Variable acceptance among pathologists for lesser confidence in diagnosis • Need of additional training • Potential delay of turn-around times

Overview of AI application in CPATH

- Hardware

- Software

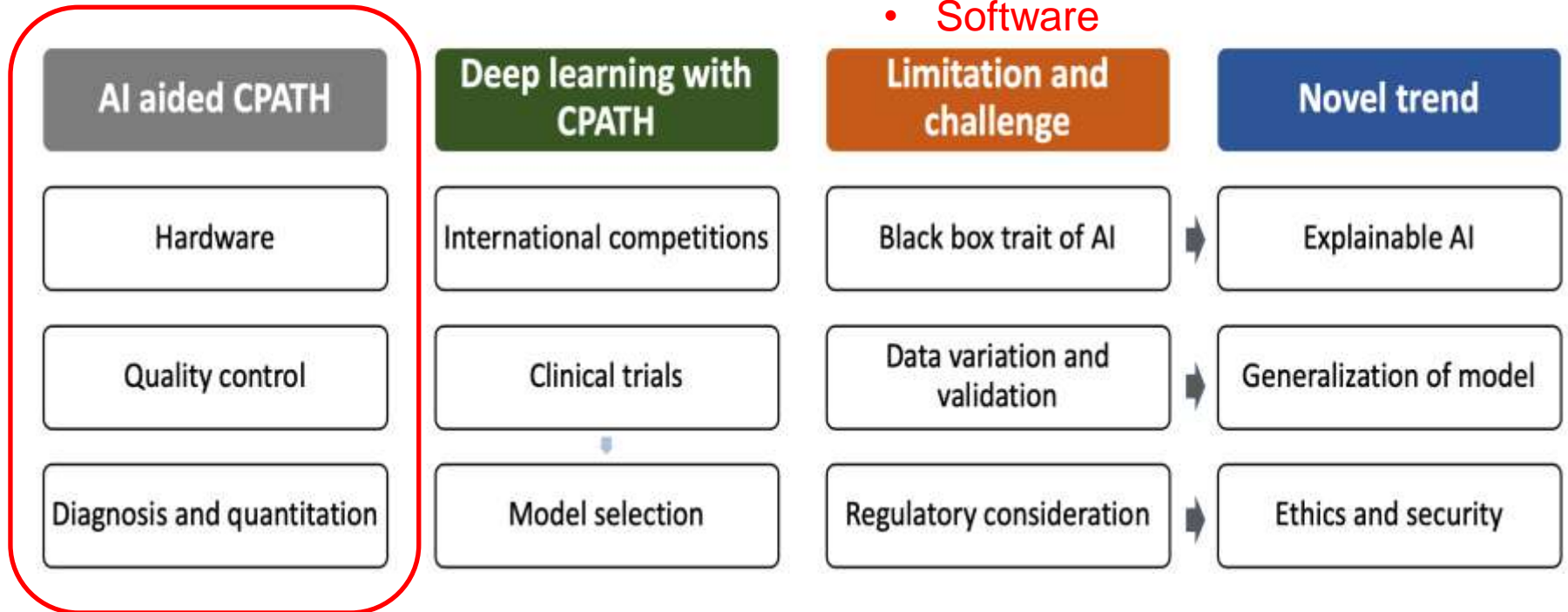
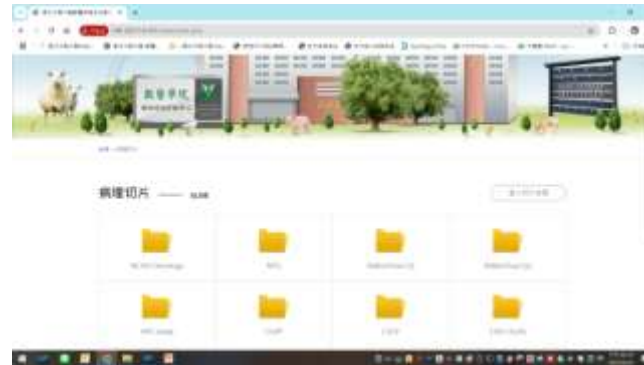


Figure 2. Requirement for clinical applications of artificial intelligence with computer pathology, CPATH

Requirements



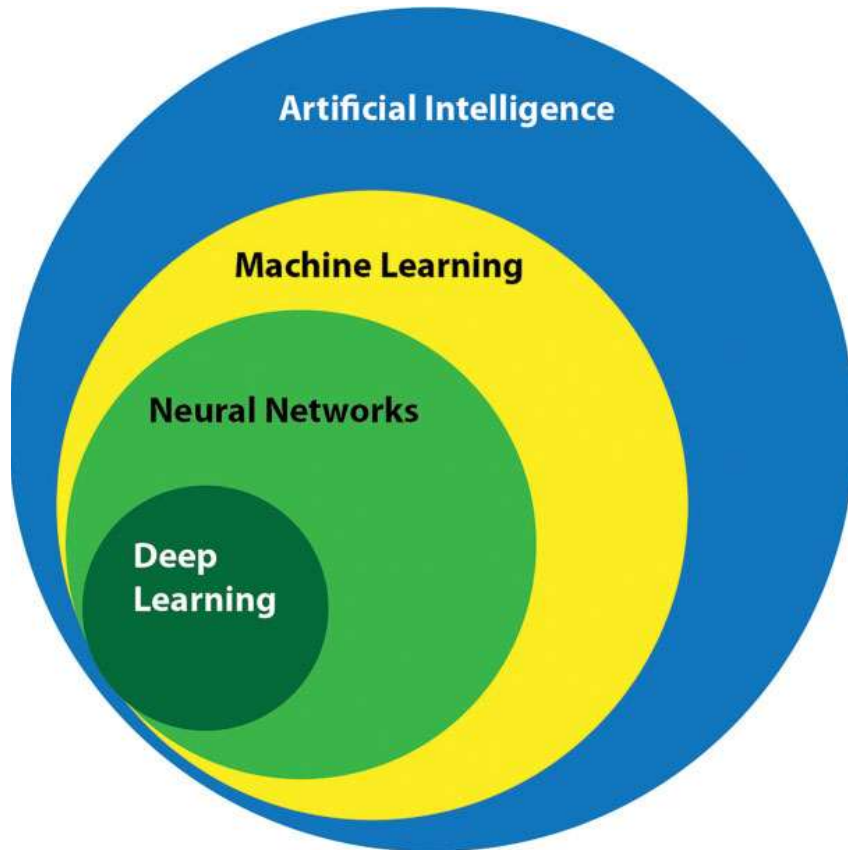
- Hardware - Fire wall, scanner (1-4 GB/WSI)...



- Hardware –
Server, High-Net, GPU
(Graphics Processing Unit,
NVIDIA...), UPS, air condition,
...

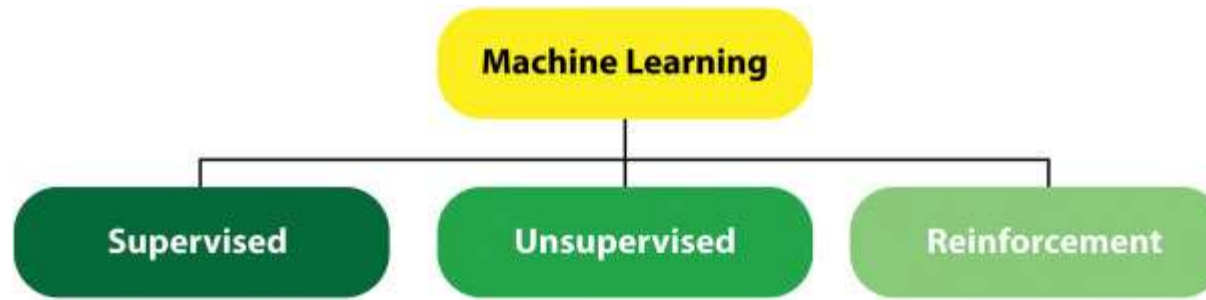
- Software - Home page, management,
models...

Software



- The term “**artificial intelligence**” was initially introduced by John McCarthy at a 1956 Dartmouth conference on AI, defined then as “**the science and engineering of making intelligent machines.**”
- It defines the more relevant terms of **AI**, **ML**, artificial neural networks (**ANNs**), and deep learning (**DL**) and their relationships with each other

Figure 1. Overview of the relationships between disciplines within the field of artificial intelligence



- 1. Supervised learning**, the computer is **provided with the features** related to the target (**input**) to train the algorithm. For example, to use supervised learning to identify a **liver**, a set of images of **normal hepatic lobules, cords, sinusoids, portal regions, and central veins** are presented to the computer and the label (i.e., liver) is provided.
- 2. Unsupervised learning** is used in instances where it **is difficult** or impossible **to define characteristic features** of biological tissues. The computer is presented with a collection of different tissues from **various organs together**
- 3. Reinforcement learning**, wherein the computer **learns from its mistakes**. In this approach, the computer is supplied with an **unlabeled input** and forced to predict the output.

AI development in pathology that will provide such opportunities include: (for tumors)

1. Distinction between **benign tissue and tumor**
2. Grading of **dysplasia and in-situ** lesions
3. Evidence and extent of **invasion**
4. Identification of **micro-metastases** in lymph node resections
5. **IHC/in-situ hybridisation scoring** of multiple biomarkers and topography of the immune response
6. **Percentage** of tumour and overall cellular content
7. Extracting new patterns from the digital images and clinical correlates (**next-generation morphology**)
8. **Automated management** and prioritization of pathology workflows

AI application in toxicologic pathology

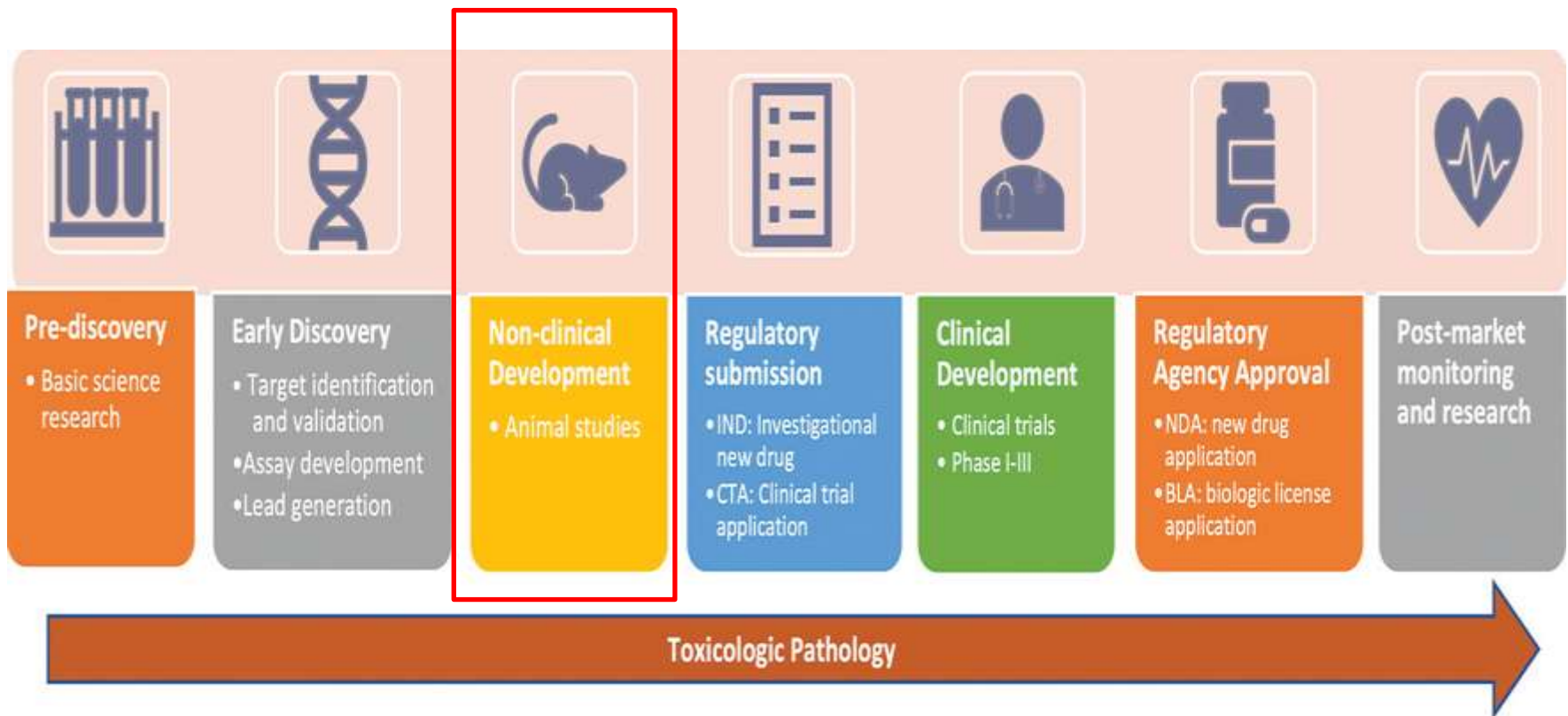


Figure 1: Drug discovery and development process.

This flowchart is a simplified version of the pipeline, and there are overlaps and close collaborations between different steps.

Example EPA/FIFRA Requirements for Hazard Evaluation of Pesticides

REVISED 870 GUIDELINE	TYPE OF TOXICITY STUDY	TEST SYSTEM	OBJECTIVE	APPROXIMATE COST/STUDY* (US\$)
1100	Acute oral	Rats	Define toxic dose by ingestion	2,700
1200	Acute dermal	Rabbits	Define toxic dose by absorption through skin	2,000
1300	Acute inhalation	Rats	Define toxic dose by inhalation	6,800
2400	Ocular	Rabbits	Assess eye irritation/injury	2,000
2500	Skin irritation	Rabbits	Assess skin irritation/injury	130
2600	Sensitization	Guinea pigs	Assess allergic potential	4,000
6100–6855	Neurotoxicity ^{†,‡}	Hens/rats	Assess nervous system injury	34,000 [†]
5100–5915	Mutagenicity [§]	In vivo/in vitro	Determine genotoxic potential; screen for carcinogenicity	6,800
3050–3465	Range-finding [§] Subacute (28- to 90-day*)	Rats	Determine effects following repeated doses; set dose level	95,000
		Mice		95,000
		Dogs	For longer studies	136,000
		Rabbits		101,000
		Rats	Identify target organs; set dose	258,000
4200–4300	Carcinogenicity/ chronic toxicity	Rats	Determine potential to induce tumors; define dose–response relationships (lifetime)	1,900,000
		Mice		1,087,000
		Dogs	Determine long-term toxic effects (1 year)	543,000
3550–3800	Reproduction and teratogenicity	Rats	Determine potential to cause fetal abnormalities and effects on development, fertility, pregnancy, and development of offspring over at least two generations	686,000
		Rabbits		
7485	Toxicokinetics	Rats, mice	Determine and quantitate the metabolic fate of a pesticide	135,000
8600	Developmental neurotoxicity	Rats	Determine potential to cause adverse developmental outcomes following exposure during gestation and lactation on gross neurological behavioral abnormalities and function, motor activity, neuropathology and brain weight measurements throughout post-natal development and adulthood	700,000

NT\$:181,662,900

Chronic and Carcinogenicity Toxicity Test

- **Rat and mouse** (oral, dermal, or inhalation)
- Control, vehicle control, and treated groups
- **Number**: 20 males and 20 females per group (**total no.: 400**)

- **Dosing**:
 - 3 dose levels (minimal, intermediate, maximal doses)
 - Interval sacrificed groups (at 6, 12, 18-mos for rats)**
 - Repeated doses treatment and a **2-year** observation period

- **Observations**:
 - Clinical signs, Mortality, Body weight change, Hematology, Gross and micro pathology, Urinary, **Tumor incidence**...

- **Data analysis**: **NOAEL, mg/kg/bw/day**

Organ trimming in chronic (2-year) study

Cassette No.*	Sex	Tissue*	No	Trimming
A1	B	前腦	1	C
		中腦	1	C
		小腦	1	C
A2	B	脊髓	3	C
		腦下腺	1	W
B1	B	眼球	2	L
		視神經	2	L
		哈氏腺	2	C
B2	B	唾液腺	3	W
		頸部淋巴結	1	W
		舌頭	1	C
B3	B	甲狀腺	2	C
		副甲狀腺	2	C
		食道	1	C
		氣管	1	C
C1	B	心臟	1	L
		主動脈	1	C
C2	B	胸腺	1	C
		肺	2	C
D1	B	胃	1	L

D2	B	十二指腸	1	C
		空腸	1	C
		迴腸	1	C
D3	B	盲腸	1	C
		結腸	1	C
		直腸	1	C
E1	B	肝	2	C
		脾	1	C
		腸繫膜淋巴結	1	W
E2	B	左腎	1	L
		右腎	1	C
		膀胱	1	L
E3	B	腎上腺	2	W
		胰臟	1	C
F1	M	前列腺	2	C
		儲精囊	2	C
F2	M	睪丸	2	C
F3	M	副睪	2	L
F4	F	子宮角	2	C
		子宮頸	1	L
		陰道	1	C

GLP lab.

20-25 blocks/rat

x 400 rats ~

10,000 slides

F5	F	卵巢	2	C
		輸卵管	2	C
		乳腺	1	L
G1	B	肌肉	1	L
		坐骨神經	1	L
		皮膚	1	L
G2	B	投藥部位	R	R
H1	B	股骨	1	L
H2	B	胸骨	1	L
H3	B	鼻甲骨 I	1	C
		鼻甲骨 II	1	C
H4	B	鼻甲骨 III	1	C
		鼻甲骨 III	1	C



Toxicologic pathology



1. Toxicologic pathology traditionally and most commonly uses **H&E-stained tissue sections** on glass slides to microscopically examine the effects of treatment on tissues **in laboratory animals**
2. A **investigational new drug (IND)**-enabling rodent study (90-day) has approximately 60 tissues for each of 80–100 animals; chronic study (2yr) of 200-400 animals. Microscopic evaluation of **thousands of slides per study** is **labor-intensive and time-consuming**
3. Years of experience and expertise are needed **to differentiate normal background lesions** – those developing spontaneously in laboratory animals due to age, sex, diet, or strain– from **drug-induced abnormalities**

Virgin albino Sprague-Dawley rats

Table 2
Summary of the most frequent anatomical pathologies observed.

Seralini et al, 2012

Organs and associated pathologies	Controls	GMO 11%	GMO 22%	GMO 33%	GMO 11%+R	GMO 22%+R	GMO 33%+R	R (A)	R (B)	R (C)
Males, in liver	2 (2)	5 (4)	11 (7)	8 (6)	5 (4)	7 (4)	15 (5)	11 (5)	9 (7)	6 (5)
In hepatodigestive tract	6 (5)	10 (6)	13 (7)	9 (6)	9 (6)	13 (6)	17 (7)	23 (9)	16 (8)	9 (5)
Kidneys, CPN	3 (3)	4 (4)	5 (5)	7 (7)	5 (5)	11 (4)	14 (4)	6 (6)	5 (5)	3 (3)
Females, mammary tumors	8 (5)	15 (7)	10 (7)	15 (8)	10 (6)	11 (7)	13 (9)	20 (9)	16 (10)	12 (9)
In mammary glands	10 (5)	22 (8)	10 (7)	16 (8)	17 (8)	13 (8)	15 (9)	26 (10)	20 (10)	18 (9)
Pituitary	9 (6)	23 (9)	20 (8)	8 (5)	11 (4)	9 (4)	19 (7)	22 (8)	16 (7)	13 (7)

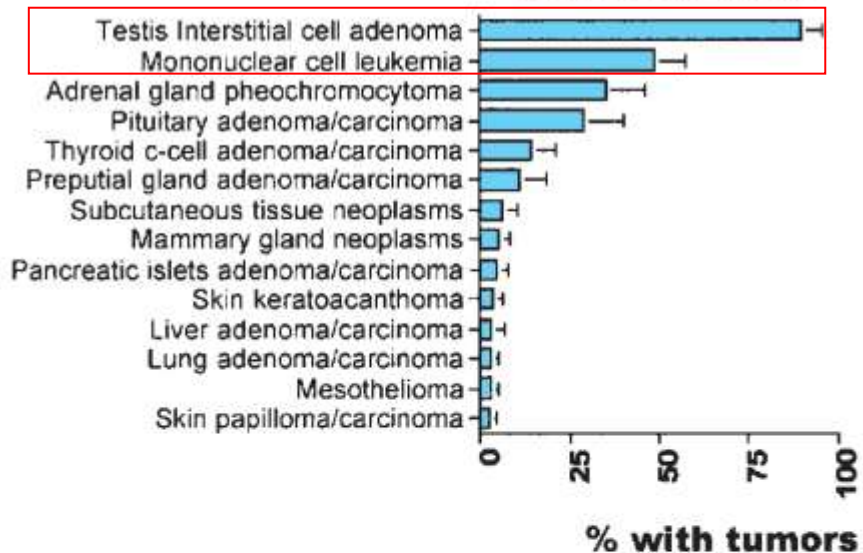
After the number of pathological abnormalities, the number of rats reached is indicated in parentheses. In all animals pathological signs are liver congestions, macroscopic spots and microscopic necrotic foci. Hepatodigestive pathological signs concern the liver, stomach and small intestine (duodenum, ileum or jejunum). Only marked or severe chronic progressive nephropathies (CPN) are listed, excluding two nephroblastomas in groups containing GMO 11% and GMO 22%+Roundup. In females, mammary fibroadenomas and adenocarcinomas are the major tumors detected; galactoceles and hyperplasias with atypia are also found and added in mammary glands pathological signs. Pituitary dysfunctions include adenomas, hyperplasias and hypertrophies. For details of the various treatment groups see Fig. 1.



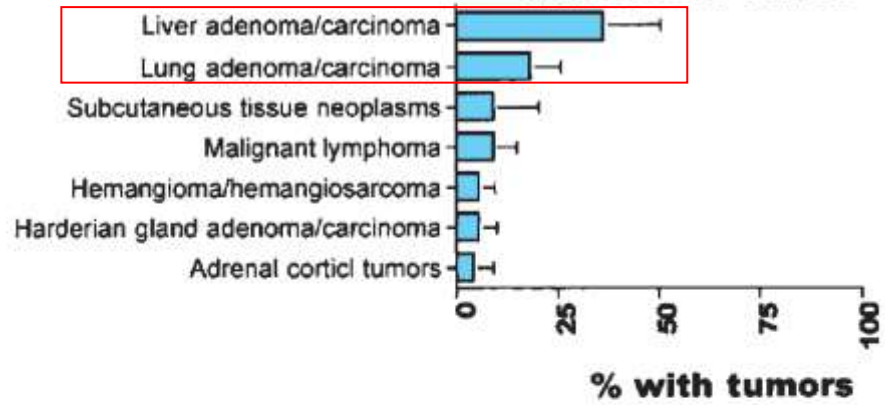
RAT MODELS

- Industry-sponsored studies generally use the **F344, Sprague-Dawley (SD), Harlan Sprague-Dawley, or Wistar rats**, the latter three most common today.
- The importance of **rat strain selection** is demonstrated by their differences in **susceptibility** to both non-neoplastic and neoplastic changes.
- For example, **mammary gland fibroadenomas** are the most common spontaneous tumor in **female SD rats**, with incidences reported as high as **70% in chronic studies**. In contrast, female **Fischer rats** have reported incidences of **about 40%**.
****Fibroadenomas are not considered a premalignant lesion in humans nor are rat mammary fibroadenomas considered predictive of carcinoma in women.**
- **Spontaneous mammary adenocarcinomas**, which are considered relevant in studies, **are more common in female SD rats**, with reported incidences of **11%**.

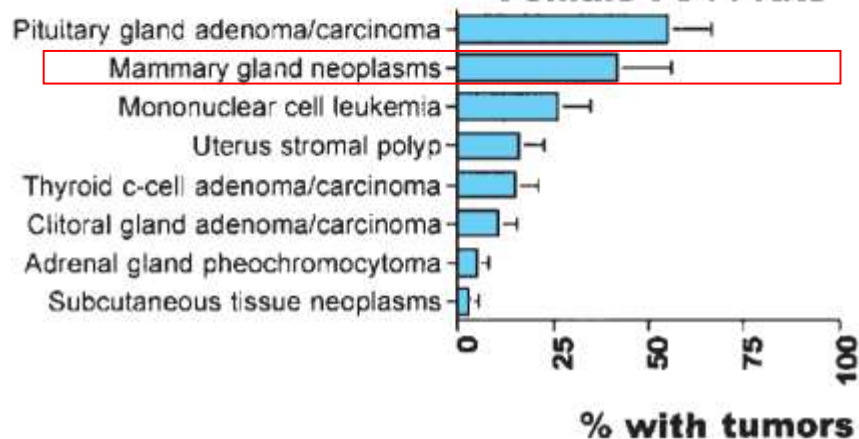
Male F344 rats



Male B6C3F1 mice



Female F344 rats



Female B6C3F1 mice

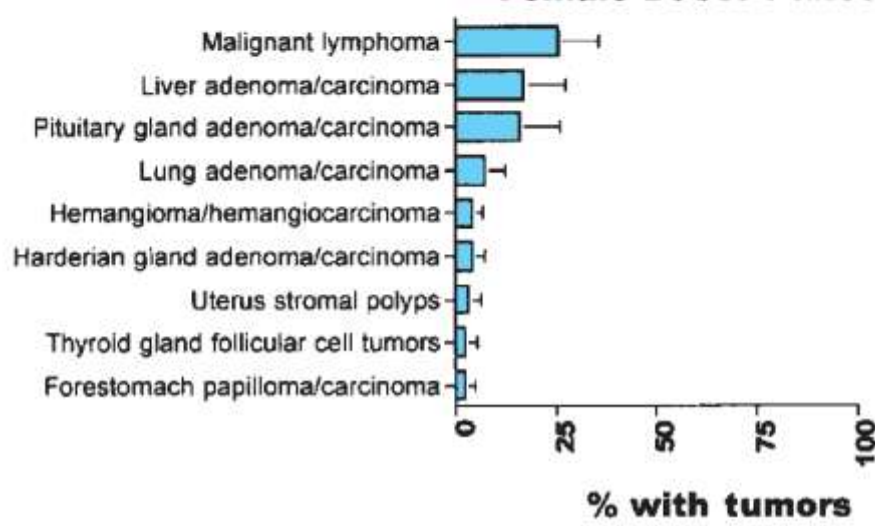


Figure 2-13. Most frequently occurring tumors in untreated control rats from recent NTP 2-year rodent carcinogenicity studies.

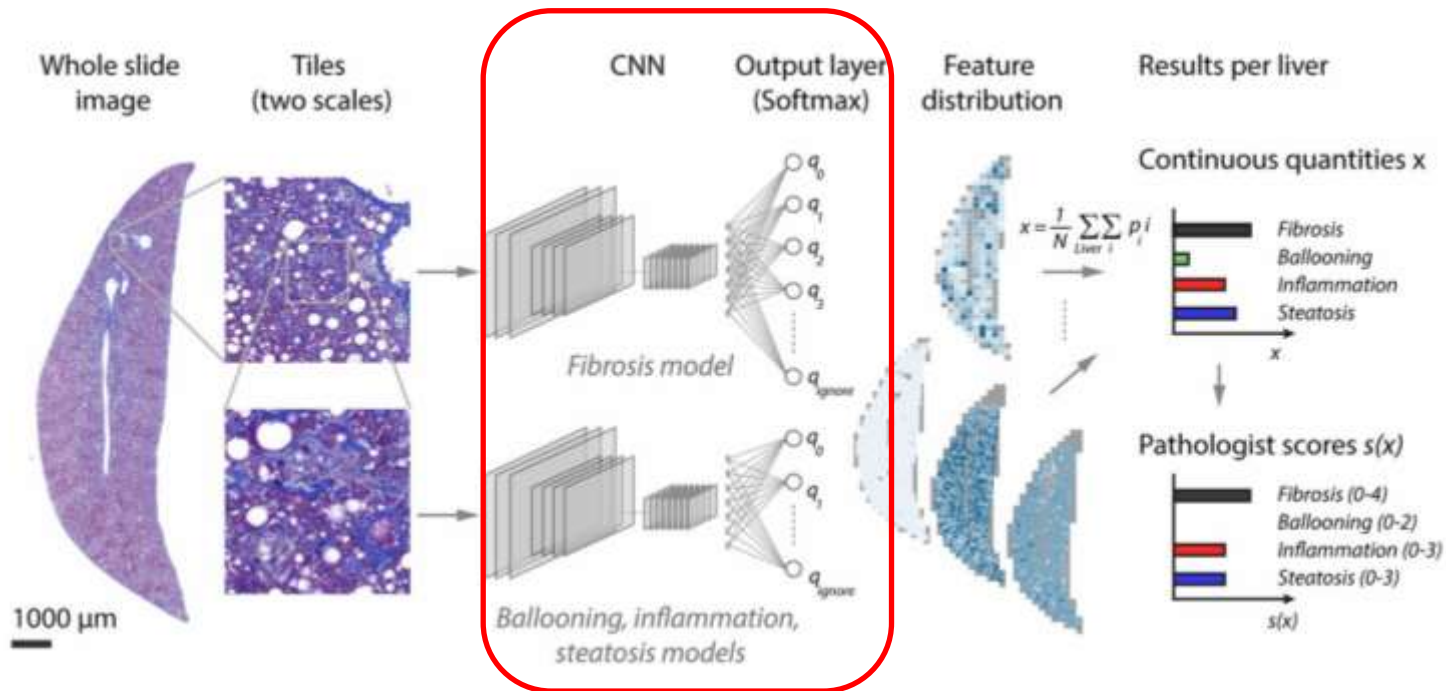
Figure 2-14. Most frequently occurring tumors in untreated control mice from recent NTP 2-year rodent carcinogenicity studies

AI-assisted analyses in nonclinical research and toxicologic pathology

Table 2: Overview of deep learning-based applications in nonclinical histopathology

Reference	Species	Tissue	Application	Method	Dataset
Nonclinical basic science research					
Bukowy <i>et al.</i> , 2018 ^[72]	Rat	Kidney	Glomeruli detection	Detection: (R-CNN)	74 kidneys, trichrome-stained
Heinemann <i>et al.</i> , 2019 ^[73]	Mouse Rat	Liver	Pathologist-like scoring of NASH models	Classification: (Inception-V3)	258 cases, trichrome-stained
Asay <i>et al.</i> , 2020 ^[74]	Mouse	Lung	Tuberculosis pulmonary pathology	Classification: (Modular CNNs)	176 slides, H & E
Yurttakal <i>et al.</i> , 2020 ^[75]	Rat	Kidney	Diabetic versus nondiabetic	Classification: (VGG19)	396 slides, H & E
Kumar <i>et al.</i> , 2020 ^[76]	Dog Human	Mammary tumor	Tumor detection	Classification: (VGG-16)	352 slides, H & E
Aubreville <i>et al.</i> , 2020 ^[77]	Dog	Skin tumor	Counting mitotic figures	Segmentation, detection, and regression: (U-Net, RetinaNet, customized CNN with ResNet50 stem)	32 cases, H & E (public dataset ^[33])
Zormpas-Petridis <i>et al.</i> , 2020 ^[78]	Human Mice	Abdominal tumor in mice	Mapping tumor heterogeneity	Classification: (Super-resolution CNN)	13 specimens, H & E

Deep learning enables pathologist like scoring of **NASH models**



Model:
Inception-v3

Figure 1. Overview of the workflow for the automated scoring of fibrosis, ballooning inflammation and steatosis, the features correlated with **non-alcoholic fatty liver disease (NAFLD)/non-alcoholic steatohepatitis (NASH)**.

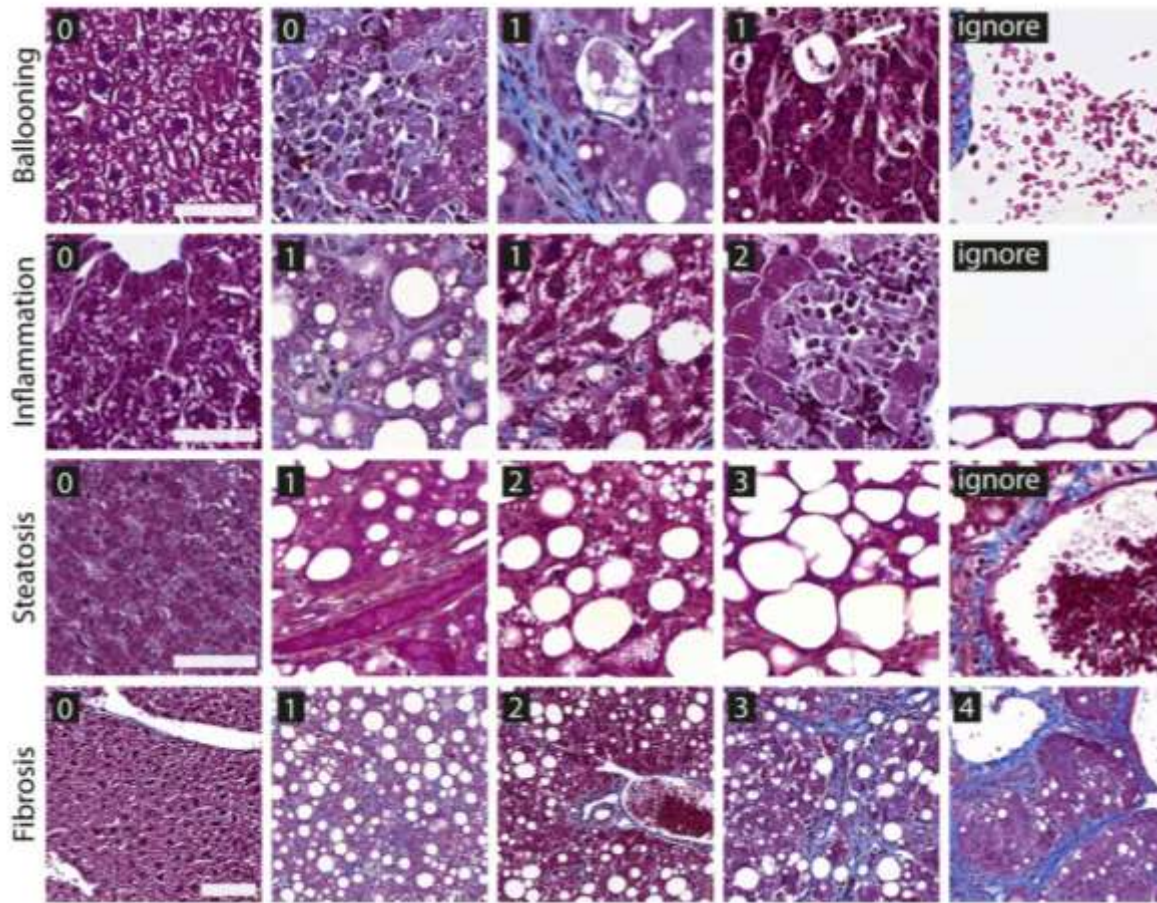


Figure 2. Examples of the classes used to train the **four convolutional neural networks (CNN)** to recognize relevant features of the **histopathological features in the Kleiner score**.

First row: ballooning, with classes 0 (no-ballooning), 1 (ballooning cells, see arrows) and ignore (insufficient liver tissue visible on a tile). Second row: inflammation with classes 0 (no inflammation), 1 (moderate inflammation), 2 (severe inflammation with clear inflammatory foci) and ignore. Third row: steatosis with classes 0 (<5% area coverage of vacuoles), 1 ($\geq 5\%$ and <33%), 2 ($\geq 33\%$ and <66%), 3 ($\geq 66\%$) and ignore. Fourth row: fibrosis with classes 0, 1 (perisinusoidal or periportal fibrosis), 2 (perisinusoidal and periportal fibrosis), 3 (bridging fibrosis), 4 (cirrhosis) and ignore (not shown). Scale bars in first three rows (high magnification tiles): 50 μm , last row (low magnification tiles): 100 μm .

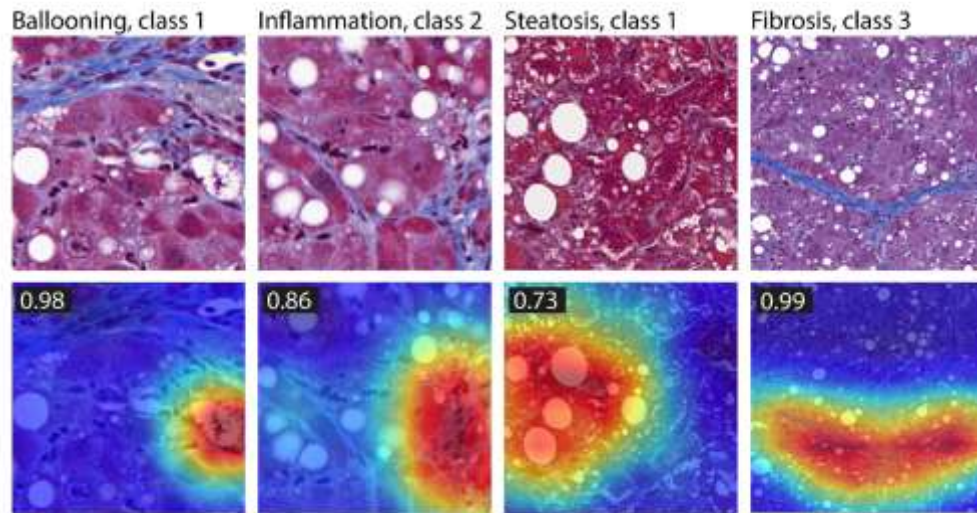


Figure 3. Examples of class activation maps for the four **convolutional neural network (CNN)** models.

Model:
Inception-v3

Table 1. Accuracy of tile classification performance of the four **convolutional neural network (CNN)** models on ballooning, inflammation, steatosis and fibrosis.

	Classification accuracy		N		Number of classes including "ignore"
	Train	Validation	Train	Validation	
Ballooning	94.0%	93.1%	13590	1555	3
Inflammation	86.2%	86.0%	8567	914	4
Steatosis	93.8%	94.5%	6377	737	5
Fibrosis	88.5%	86.3%	4251	465	6

N is the number of labeled tiles used for training and validation.

AI-assisted analyses in nonclinical research and toxicologic pathology

Table 2: Overview of deep learning-based applications in nonclinical histopathology

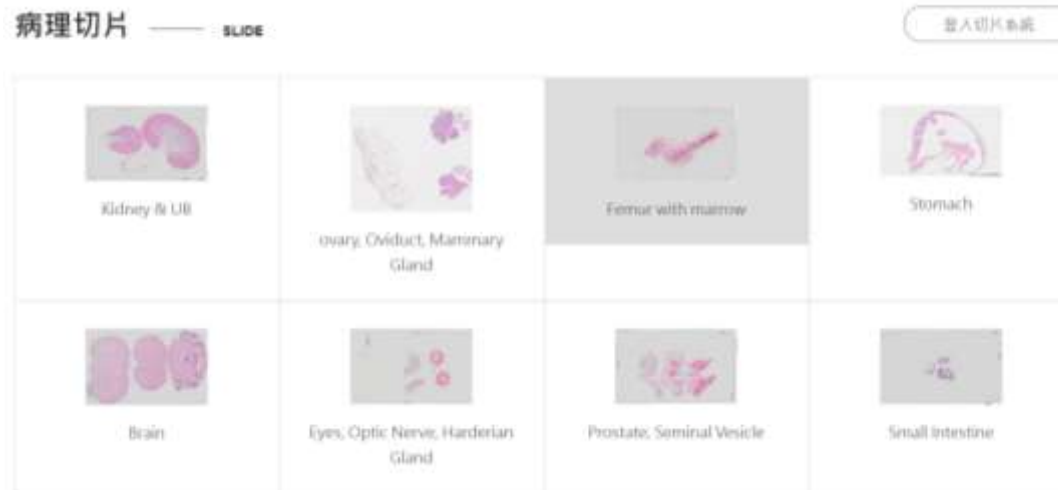
Reference	Species	Tissue	Application	Method	Dataset
Sonigo <i>et al.</i> , 2018 ^[81]	Mouse	Ovary	Ovarian follicle counting	Classification: (CNN inspired by VGG19)	194 slides, H & E
Yu <i>et al.</i> , 2018 ^[82]	Rat	Liver	Liver fibrosis staging	Classification: (AlexNet)	25 rats, collagen-stained
Horai <i>et al.</i> , 2019 ^[67]	Not mentioned	Liver Kidney Thymus Skeletal muscle Spleen Adipocyte Parotid gland Sublingual gland Adrenal gland	Quantifying specific histopathological findings such as vacuolation, hypertrophy, bile duct proliferation, and necrosis in liver	Segmentation: HALO (image analysis, such as filters and shape distinction and random forest*)	Not mentioned
Hu <i>et al.</i> , 2020 ^[83]	Rat	Ovary	Ovarian toxicity assessment based on corpora lutea count	Detection: (Model based on RetinaNet)	224 slides, H&E
Hoefling <i>et al.</i> , 2021 ^[32]	Rat	46 different tissue types	Normal histology	Classification: (VGG-16, Inception-V3, ResNet-50)	1690 slides, H & E
Rudmann <i>et al.</i> , 2021 ^[84]	Mouse	Lung Thymus Stomach	Carcinogenicity	Segmentation: Deciphex (inception, resnet-50 efficientnet)	170 slides, H & E
Pischon <i>et al.</i> , 2021 ^[86]	Rat	Liver	Hepatocellular hypertrophy quantification	Segmentation: visiopharm (U-Net)	28 slides for training, H & E
Mudry <i>et al.</i> , 2021 ^[87]	Rat	Eye	Retinal atrophy evaluation	Segmentation: MATLAB (VGG-16)	112 rats, H & E

Normal-histo-rat

切片連結 <http://140.120.114.107/slidecenter.php>

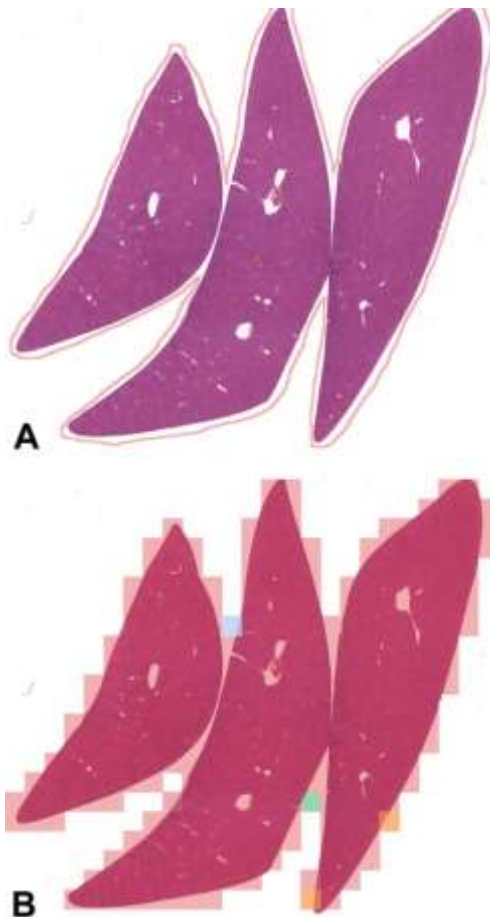


切片連結 <http://140.120.114.107/slidecenter.php?id=69>



HistoNet: A Deep Learning-Based Model of Normal Histology

Toxicologic Pathology
2021, Vol. 49(4) 784-797
© The Author(s) 2021
Article reuse guidelines:
sagepub.com/journals-permissions
DOI: 10.1177/0192623321993425
journals.sagepub.com/home/tpx



1. On **1690 slides** with rat tissue samples from 6 preclinical toxicology studies, tissue regions were outlined and annotated by pathologists into 46 different tissue classes.
2. Using 4 studies as training set and 2 studies as test set, we trained **VGG-16, ResNet-50, and Inception-v3 networks** separately at each magnification level.
3. Among these model architectures, Inception-v3 and ResNet-50 outperformed VGG-16. **Inception-v3** identified the tissue from query images, with **an accuracy up to 83.4%**.
4. Most **misclassifications** occurred between histologically **similar tissues**.

Model Interpretation

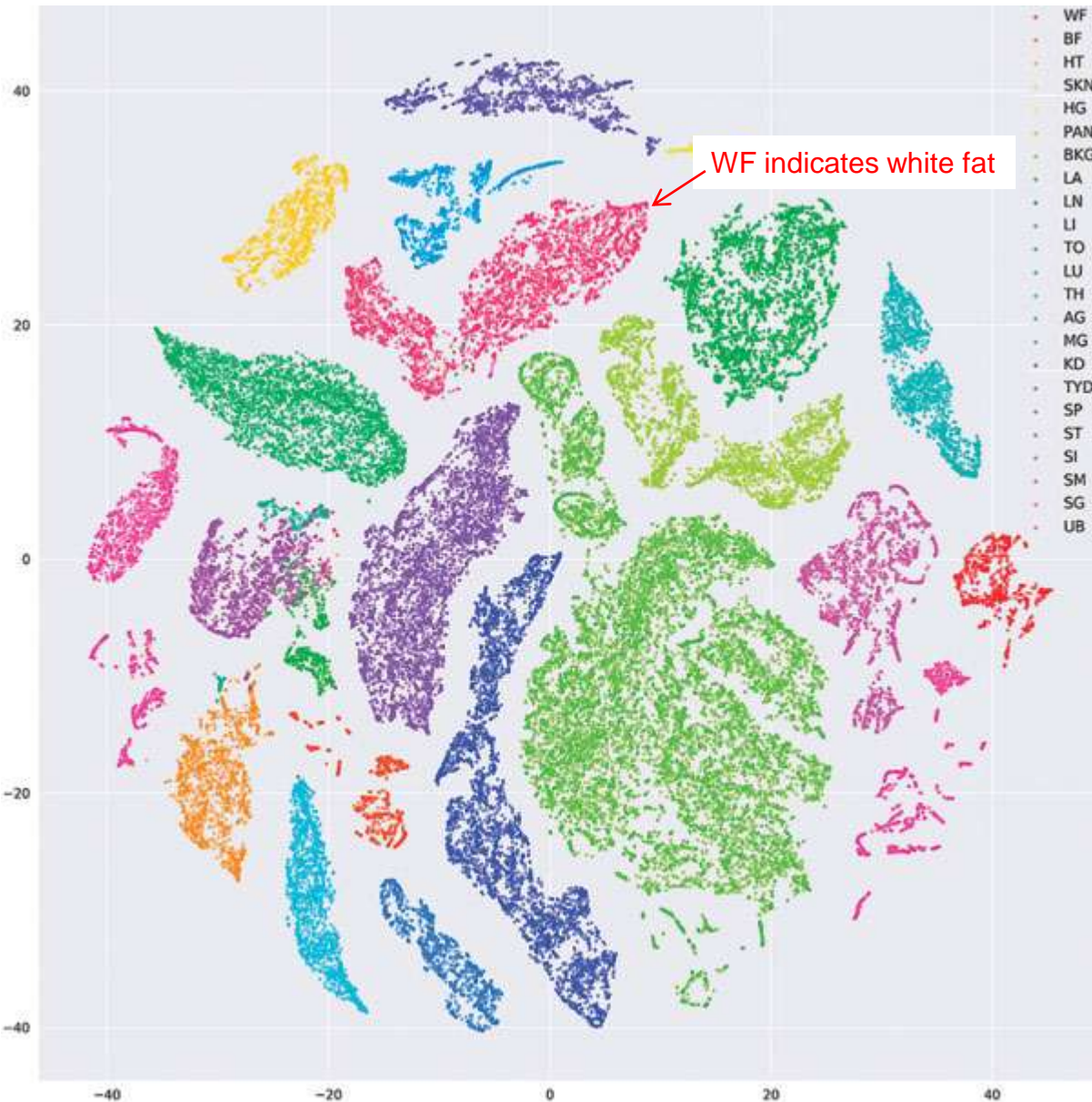


Figure 4. **t-Distributed Stochastic Neighbor Embedding (t-SNE)** visualization of the embedding space learned by a neural network trained to **recognize rat tissues of different types**. Each point in this plot corresponds to a small image patch that is color-coded according to its true tissue type. Each cluster and color represents a different tissue. Most points are within distinct, non-overlapping clusters.

WF indicates white fat; BF, brown fat; HT, heart; SKN, skin; HG, Harderian gland; PAN, pancreas; BKG, background; LA, large intestine; LN, lymph node; LI, liver; TO, tongue; LU, lung; TH, thymus; AG, adrenal gland; MG, mammary gland; KD, kidney; TYD, thyroid gland; SP, spleen; ST, stomach; SI, small intestine; SM, skeletal muscle; SG, salivary gland; UB, urinary bladder. Figure provided courtesy of Sing.

Example 1:

Artificial Intelligence in Toxicologic Pathology: Quantitative Evaluation of Compound-Induced **Hepatocellular Hypertrophy in Rats**



Table I. Summary of Study Protocol Differences (Test Set).^{19a}

Study number	Study I
Study subtype	7 Day
Groups: test article and dose; Subgroups: duration	Control (0 mg/kg)
	Phenobarbital (80 mg/kg)
Number of animals	15 + 15
Sex	Female
Strain	CrI: WI(Han)
Test data for algorithm	Cytoplasmic area only

Histopathological Image Analysis

- Slides were digitized, after different periods of being archived, using a **digital slide scanner** (Aperio AT2, Leica Biosystems Imaging, Inc). Slides were scanned with a **20x** objective lens (20x/0.75 NA Plan Apo) at resolution 0.5 microns/pixel.
- **Visiopharm software** (version 2020.01 and 2020.03, Denmark) was used to train the deep learning networks for development of our AI algorithms.

Pischon et al., *Toxicologic Pathology* 49(4), 2021

AI algorithm

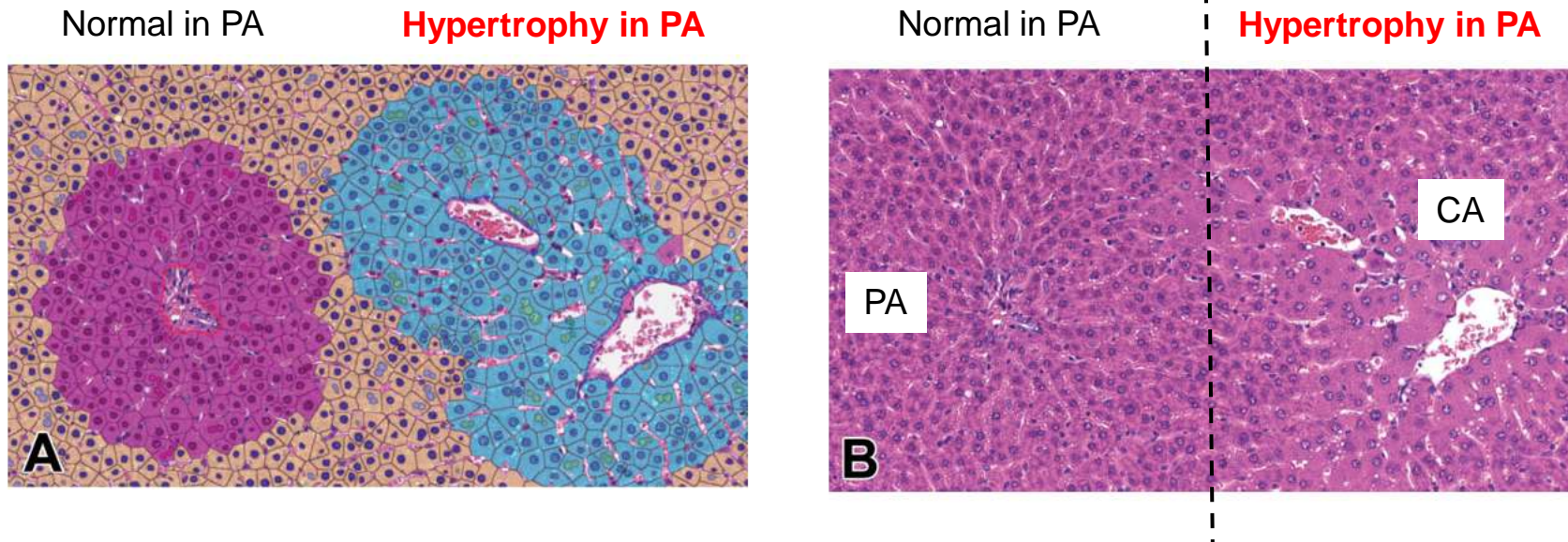


Figure 1. Segmentation achieved by AI algorithm resulting in mean cytoplasmic area measurements. Liver, H&E, original scan 20x, phenobarbital (PB)-treated study.

A, Classification as false colored overlay: hepatocellular cytoplasm according to zones (**centrilobular** cyan, midzonal yellow, **periportal** magenta), hepatocellular nuclei in darker color according to zones, binucleated cells in lighter color according to zones (only if 2 nuclei connecting), portal tract surrounded by red dashed line, **central vein** surrounded by blue dashed line, sinusoids no false color. B, Original H&E image. AI indicates artificial intelligence; H&E, hematoxylin and eosin.

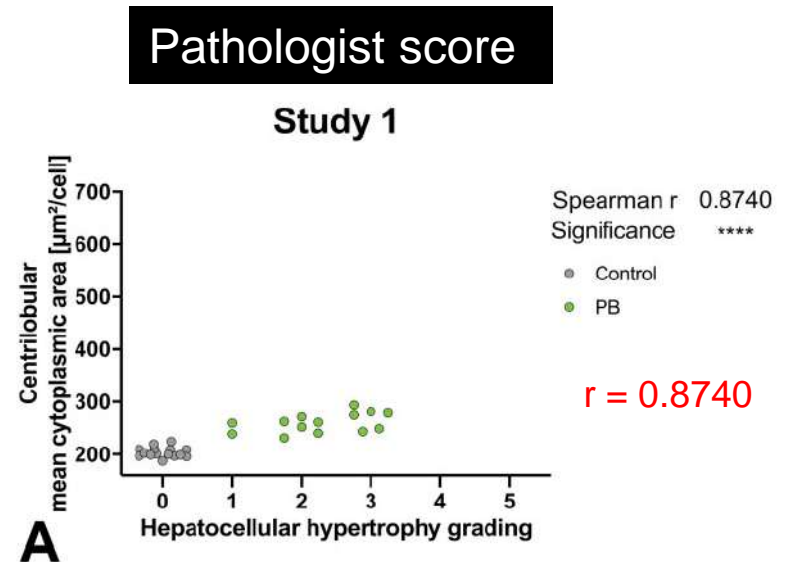
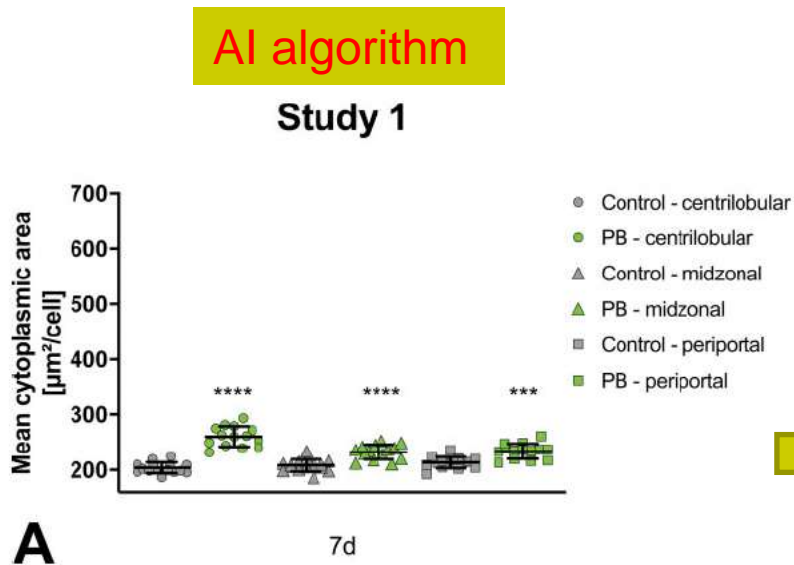


Figure 2. Hepatocellular mean cytoplasmic area **measured by AI algorithm**. Phenobarbital (PB)-treated groups (green or blue) statistically compared to control groups (gray) for respective liver zones (centrilobular sphere, midzonal triangle, periportal square)

Figure 3. Correlation of **centrilobular hepatocellular** mean cytoplasmic area **measured by AI algorithm** to semiquantitative histopathologic observation with grading done **by pathologists**.

Example 2:

Artificial Intelligence in Toxicological Pathology: Quantitative Evaluation of Compound-Induced Follicular Cell Hypertrophy in Rat Thyroid Gland Using Deep Learning Model



Table 1. Summary of Study Protocol Differences (Test Set).^a

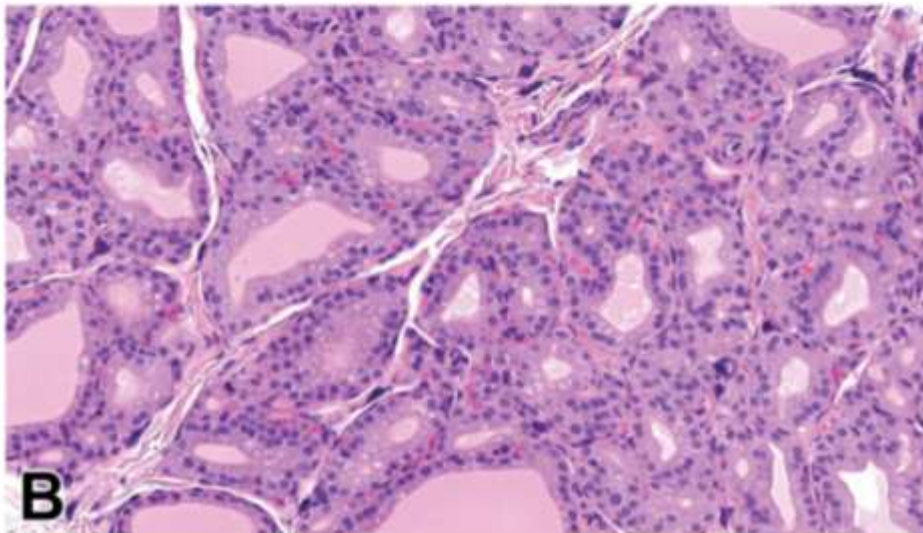
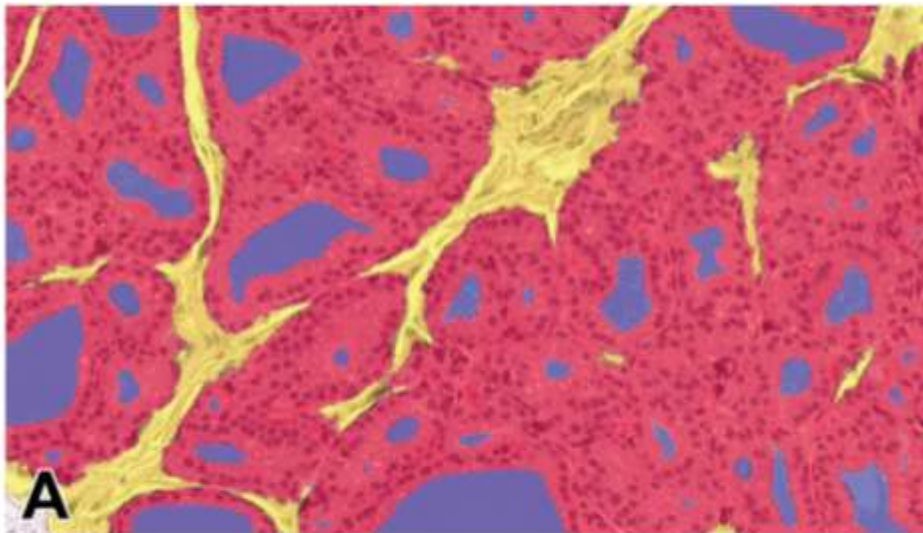
Study number	Study 1	
	14 Days	
Groups:	Control	3 Days
test article and dose;	(0 mg/kg)	7 Days
Subgroups:		14 Days
duration	Phenobarbital (80 mg/kg)	3 Days
		7 Days
		14 Days
Number of animals	14+14+14 + 14+14+14	
Sex	Male	
Age at study start→end	~8→10 weeks	
Strain	Cri:WI (Han)	
Test data for algorithm:	Cytoplasmic area + Hypertrophy area	

Histopathological Image Analysis

- Digitization was performed after slides had been archived for different time intervals, using a digital slide scanner (**Aperio AT2**, Leica Biosystems Imaging, Inc) with its 20 objective lens (20x /0.75 NA Plan Apo) at resolution 0.5 micron/pixel.
- **Visiopharm software** (version 2020.01 and 2020.03, Denmark) was used to develop DL models and train the algorithms.

Hypertrophy in Rat Thyroid Gland

Figure 1. Segmentation achieved by DL algorithm resulting in mean cytoplasmic area measurements. Thyroid gland, H&E, sodium perchlorate (SP)-treated (3 days) study 4.



A, Classification as false colored overlay: follicular epithelium in red, colloid in blue, stroma in yellow, nuclei segmentation not shown here. B, Original H&E image.

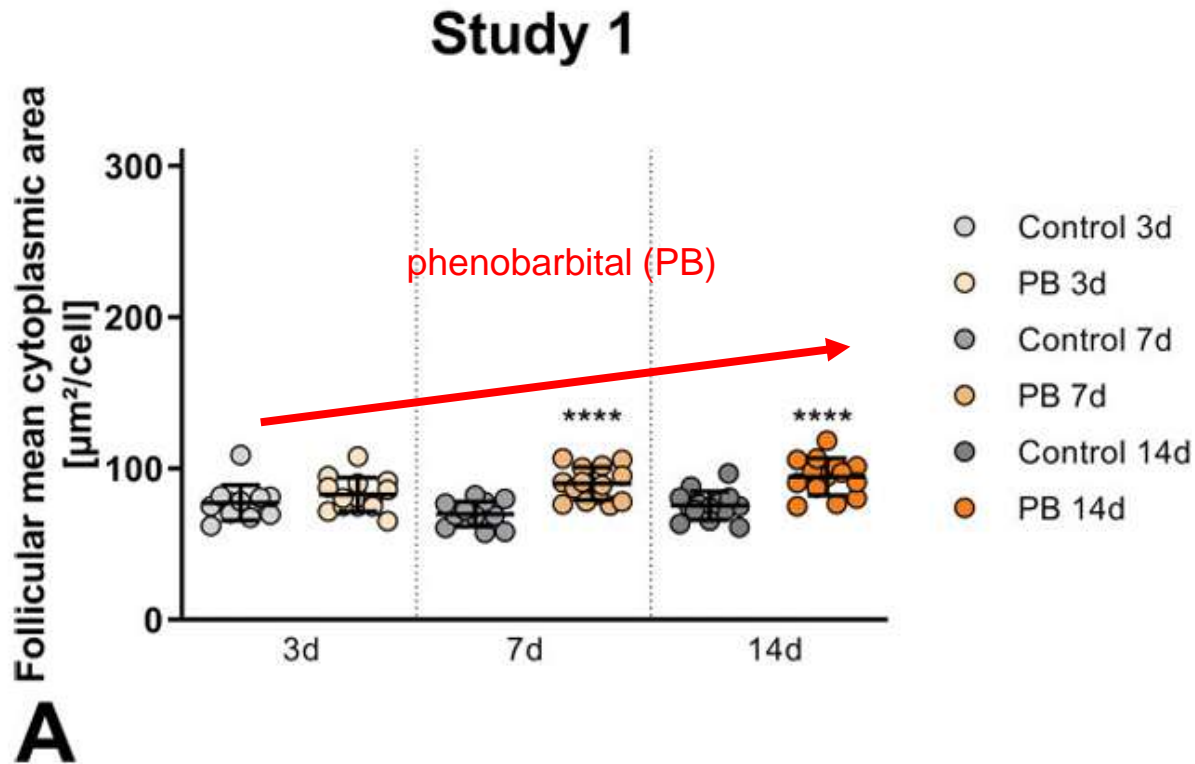


Figure 2. Follicular mean cytoplasmic area measured by DL algorithm.

Note color scheme in the respective legend indicating different reference compounds (colors) versus control (gray) groups. For study 1 (A) with phenobarbital (PB), individual values and group- or subgroup-means with standard deviation are shown. Each treated group is statistically compared to its respective control group, significant differences shown as asterisks in the graph. Linear trend analysis for dose dependent effects shown in upper right corner of respective graph.

Example 3:

Using Artificial Intelligence to Detect, Classify, and Objectively Score Severity of Rodent Progressive Cardiomyopathy (PCM)

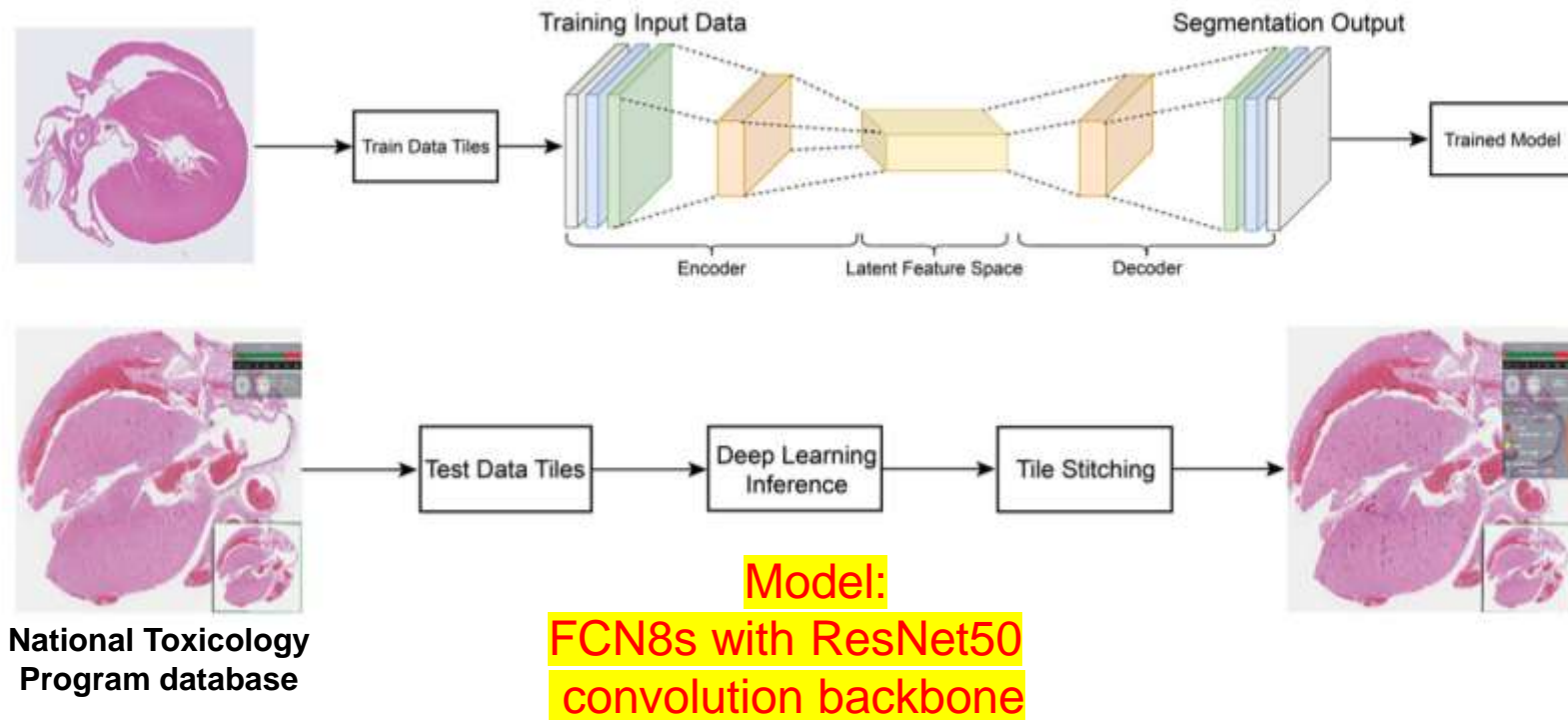


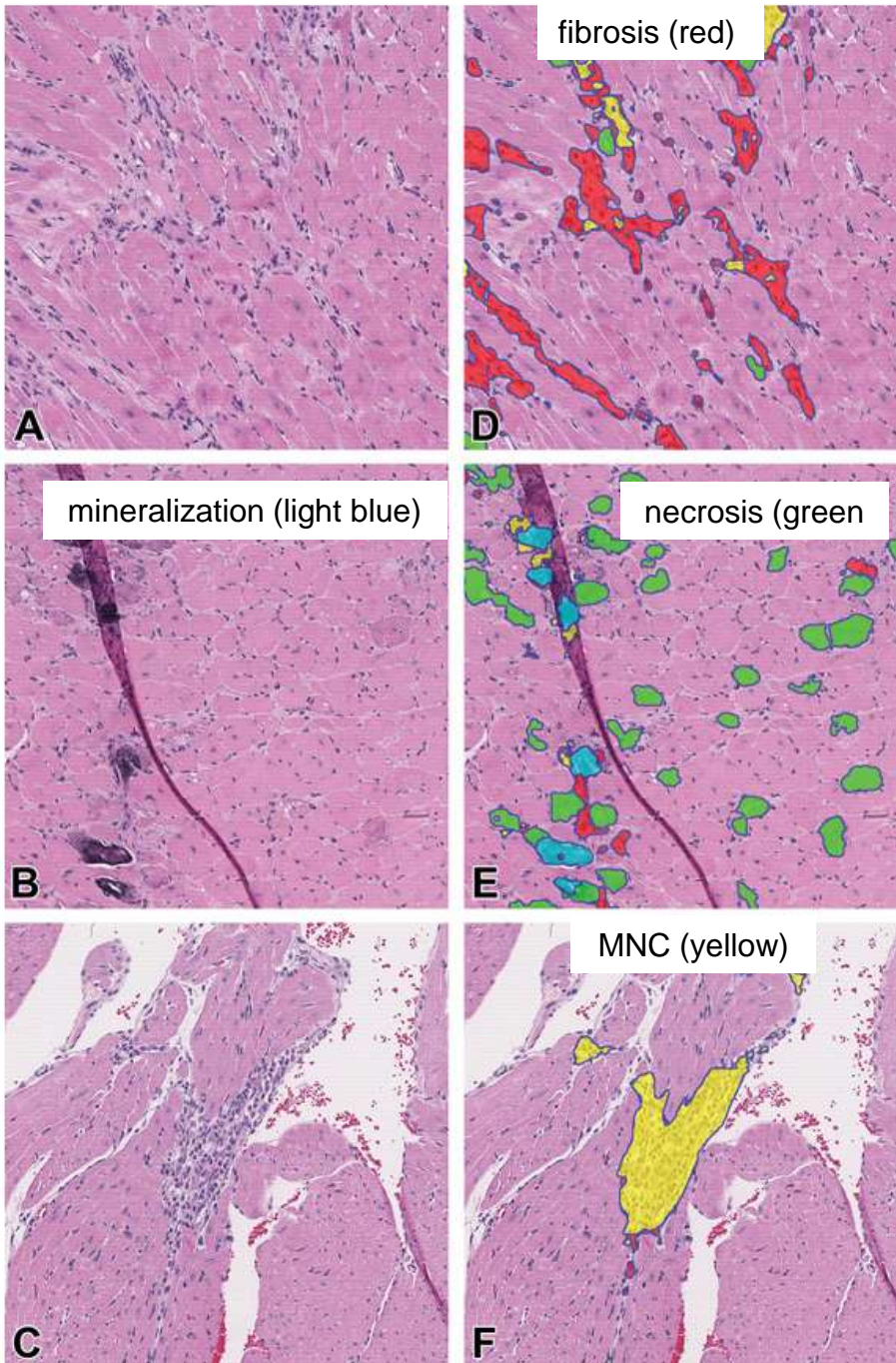
Figure 2. Cardiomyopathy algorithm training and testing pipeline. The WSIs of heart sections from Sprague Dawley rat hearts were divided into tiles of size 512 512 pixels.

Progressive cardiomyopathy (PCM)

Figure 6. Sprague Dawley rat heart images before and after algorithm segmentation.

A-C, Input images demonstrate microscopic features of PCM. D-F, The corresponding images following segmentation by the algorithm. Colored regions indicate areas predicted by the algorithm to have **fibrosis (red)**, **necrosis (green)**, **mineralization (light blue)**, and **MNC (yellow)**.

Appropriate segmentation occurred even in areas of tissue fold artifact (E). H&E, original scan 5X. H&E indicates hematoxylin and eosin; MNC, mononuclear cell infiltration; PCM, progressive cardiomyopathy.



Progressive cardiomyopathy (PCM)

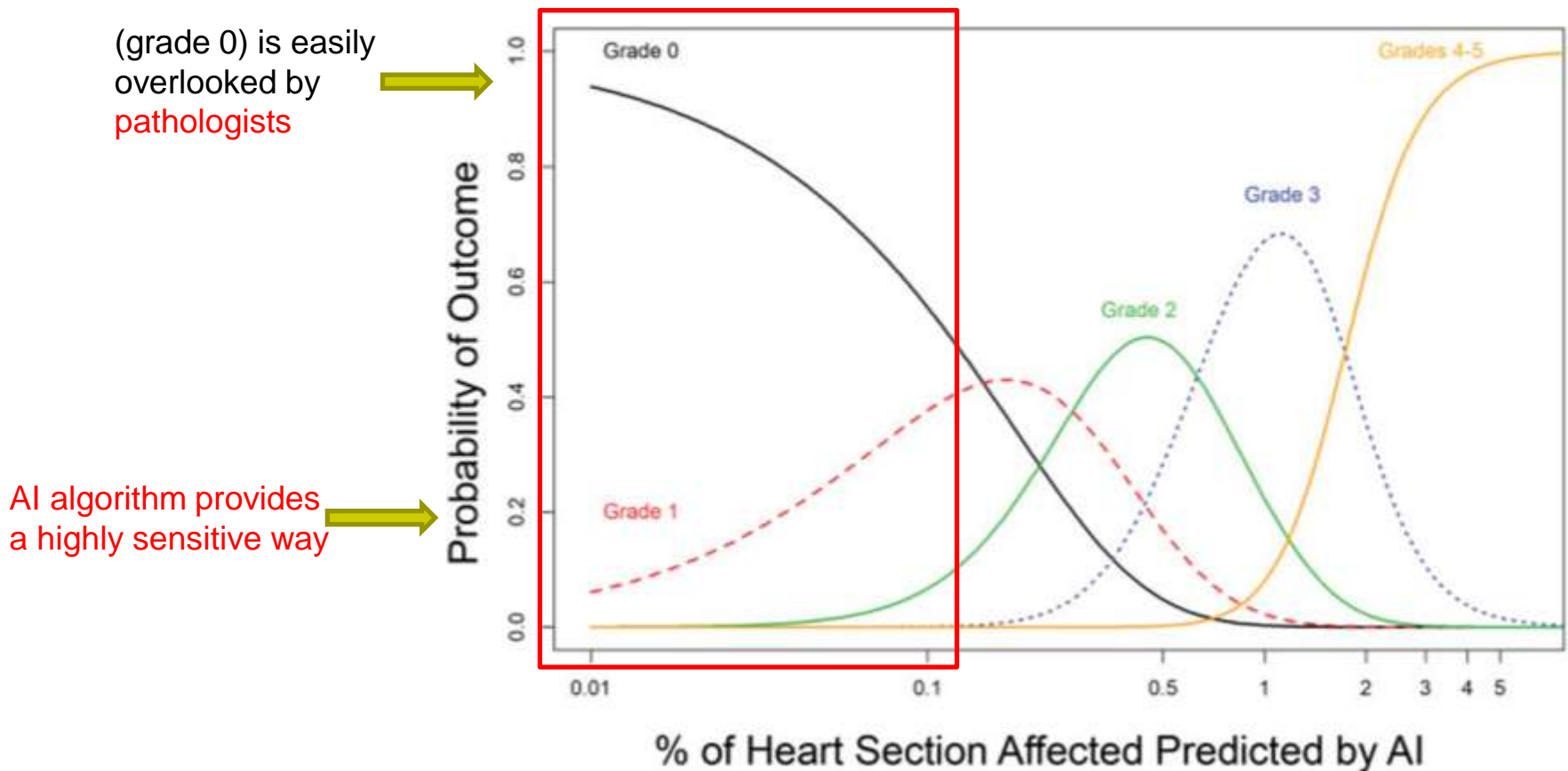
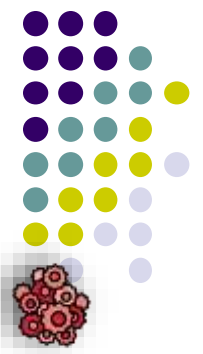


Figure 7. Predicted probabilities of grade outcomes for given AI scores based on a multinomial logistic regression model of median grade as a function of the log₁₀-transformed AI scores. AI indicates artificial intelligence; LOESS, local polynomial regression.

台灣AI數位病理發展現況

CDE, 楊清淳, 2021。

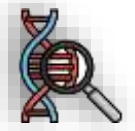


1. AI 血癌骨髓抹片之判讀

以AI完成自動計數及分類骨髓血液細胞的優點為可縮短計數時間且提高判讀的一致性。國內有**台大醫院**、**雲象科技**、**柏瑞醫**、**長庚**人工智能核心實驗室等單位著手進行研發。

2. AI 癌症病理切片之判讀

包含有乳癌、肺癌、肝癌、腦癌、卵巢癌、胃癌等判讀軟體的研發。**清大生科**、**捷絡**、**諾倫**科技等觀察及定量癌細胞的細胞核、細胞質及標靶分子(如HER2)等特徵。



3. AI 子宮頸癌抹片之判讀

僅適用以Liquid-based Specimen (LBS) 技術來處理子宮頸抹片的樣本，且演算法僅可挑選出高風險的視野，需醫事人員進行的判讀。國內的**柏瑞醫**、**影豹**智慧科技等研發單位



4. AI 微生物/基因分子病理檢測

林口長庚醫院、**長庚大學**及**中央大學**共同研發AI「超級細菌預測模型」，快速正確進行微生物特性鑑定，以增加臨床用藥之準確性。**華碩**、**高醫**及**行動基因**等單位，共同開發「AI醫療大數據搜尋系統」，協助醫師快速檢索患者腫瘤基因突變資訊



• 小鼠急性肝損傷病理輔助診斷系統開發、測試及其使用情境探勘

收集小鼠肝損傷檢體影像與病理判讀所需資訊(含圈選資料)，提供病理輔助診斷系統開發、測試、優化及使用情境探勘所需資源。**中興大學**與**XXX**等研發單位(2016)。



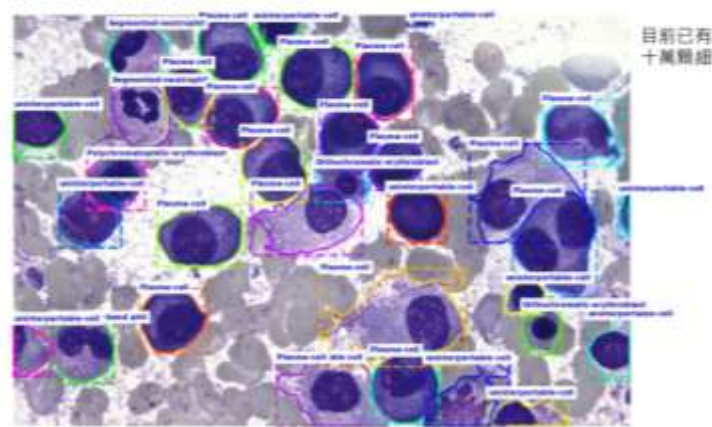


臺大醫院健康電子報 2022年04月173期

https://epaper.ntuh.gov.tw/health/202204/special_3_1.html

台大醫院、雲象科技

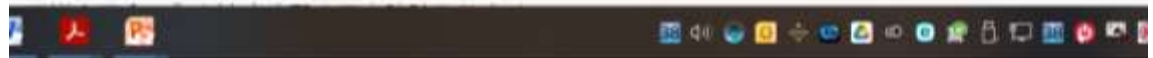
骨髓抹片影像標註範例



aetherAI
目前已有超過一百五十萬顆細胞的標註



獲衛福部歐盟核准「骨髓抹片AI分類計數」 臺大醫院與雲象科技暨立醫藥界標竿 商轉創新醫材視訊
臺大醫院與雲象科技宣布，共同研發的「骨髓抹片AI分類計數 aetherAI Hema」已獲衛福部與歐盟CE核准，是該領域全球首例同時獲兩地認證的AI醫材。「骨髓抹片AI分類計數」將一改骨髓抹片細胞人工計數作業，數，快速提供量化、可反覆驗證、客觀一致性的數據，協助醫師判讀，提升精準醫療，且可望因取證商轉應





捷絡獲首張TFDA軟體醫材證！成國內首款可離線版「數位病理平台」

撰文 | 記者 巫芝岳

日期 | 2024-01-08

 Select Language 

今(8)日，捷絡生技宣布其首款第二等級軟體醫材「捷絡數位病理影像平台」，已獲台灣衛福部食藥署(TFDA)軟體醫材許可證，成為國內首款可離線使用的數位病理產品。

該款數位病理影像平台，是運用醫療器材等級全景玻片影像軟體，可搭配體外診斷醫療器材(IVD)規格的數位病理掃片機，協助醫師進行精準診斷。

捷絡林彥穎執行長表示，這項產品為單機化設計，整合的軟硬體可安裝於邊緣運算設備獨立使用，例如個人電腦或筆記型電腦等，因此更貼近臨床診斷流程。

同時，該產品也正向美國食品藥物管理局(FDA)遞送510(k)上市前通知申請中，預計今年下半年可望取得核准。

捷絡這款數位病理影像平台，不但是公司首張取得的國內醫材證的產品，成為公司重要里程碑外，也是國內獲批的第一款可離線使用的數位病理產品。

專注於數位病理影像技術的捷絡生技，成立於2018年底、2021年進駐竹北生醫園區。其3D智慧病理影像技術，在肺癌、乳癌、前列腺癌、腸癌組織型態辨識、與腫瘤標靶分子(PD-L1、HER2)檢驗等，已累積多項研發成果，並獲產學研專家肯定。

捷絡表示，他們已在公司建構「先進病理知識管理」生態系，今年更推出智慧病理管理系統、邊緣數位病理分析系統及數位病理驗證平台等產品，並已在數個國內醫學中心與馬來西亞教學醫院投入應用。

此外，捷絡亦積極鏈結高階螢幕產業鏈，與科技業合作夥伴共同推廣適用於病理影像診斷的「專業級螢幕」。

(報導/巫芝岳)

<https://news.gbimonthly.com/tw/article/show.php?num=64186>

數位病理系統於醫療器材應用之研發策略指導原則

作者：楊孟庭

成果歸屬計畫名稱：113 年度「醫藥衛生技術評估科技發展計畫」

執行單位：財團法人醫藥品查驗中心醫療器材組

- 整理我國及歐美等國家之數位病理相關醫材的公開資料
- 分析闡明此類新興醫材之特性、優點和限制
- 歸納研發時應注意的醫療市場需求、軟硬體技術特點、法規評估重點等
- 提出產品申請我國查驗登記時，準備技術性、安全性與功能性資料之法規建議

表二、我國之已上市數位病理系統醫療器材之代表性產品

項次	1	2	3	4
產品名稱	“飛利浦”數位病理系統 (“PHILIPS” Philips IntelliSite Pathology Solution)(PIPS) (備註：美國亦取得上市許可)	“雲象”數位病理影像平台 (“aetherAI” Digital Pathology System)	“捷絡”數位病理影像平台 (“MetaLite DX” Digital Pathology Software)	“美麗佳”自動血液影像分析儀 (“Medica” EasyCell Complete System)
許可證號	衛部醫器輸字第 032394 號	衛部醫器製字第 006777 號	衛部醫器製字第 007622 號	衛部醫器輸字第 025556 號
核准上市年份	2019	2020	2023	2013
分類品項	B.1860 免疫病理組織化學試劑與套組	B.9999 其他	B.3700 病理玻片影像系統	B.5260 自動細胞定位裝置
風險等級	2	2	2	2
預期用途/ 適應症	本產品是一個自動化數位玻片建立、檢視及管理系統。PIPS 適合體外診斷使用，旨在協助病理科醫師審查及判讀由福馬林固定石蠟包埋(FFPE)組織製備之外科病理學玻片的數位影像。本產品專用於對適合以傳統光學顯微鏡手動觀察的玻片	本產品是一個醫療器材軟體，須與 Aperio AT2 DX 玻片掃描器 (Leica Biosystems Imaging, Inc.)一起使用，用於查看和解釋由福馬林固定石蠟包埋(FFPE)組織製備的手術病理玻片數位影像。本產品的功能包括在玻片上可平移以檢查所有組織區	本產品是一個醫療器材軟體，用於查看由福馬林固定石蠟包埋(FFPE)組織製備的手術病理玻片，經玻片掃描器數位化後的影像。本產品的功能包括可平移影像以檢查所有組織區域，放大與縮小影像，及於瀏覽過程中，對影像進行標註。	本產品是從固定並染色好的周邊血液抹片得到的白血球、紅血球和血小板，定位細胞並顯示圖像，利用這些圖像幫助合格的技術人員進行白血球分類、紅血球型態評估以及血小板估算。僅供體外診斷使用，僅供專業用途使用。

表三、美國之已上市數位病理系統醫療器材之代表性產品

項次	1	2	3	4
產品名稱	Philips IntelliSite Pathology Solution (備註：我國亦取得上市許可)	MMPC-4127F1	FullFocus	Paige Prostate
申請形式	De Novo、510(k)	510(k)	510(k)	De Novo
De Novo/ 510(k)號 碼	DEN160056、K172174、 K192259	K172922	K201005	DEN200080
核准上市 年份	2017、2017、2019	2017	2020	2021
法規號碼	864.3700 全玻片影像系統 (Whole slide imaging system)	864.3700 全玻片影像系統 (Whole slide imaging system)	864.3700 全玻片影像系統 (Whole slide imaging system)	864.3750 數位病理學輔助用軟 體演算法裝置 (Software algorithm device to assist users in digital pathology)
產品代碼	PSY 全玻片影像系統 (Whole slide imaging system)	PZZ 數位病理顯示器 (Digital pathology display)	QKQ 數位病理影像瀏覽和管 理軟體 (Digital pathology image viewing and management software)/ PSY 全玻片影像系統	QPN 數位病理學輔助用軟體演 算法裝置 (Software algorithm device to assist users in digital pathology)

ChatGPT in Veterinary Medicine

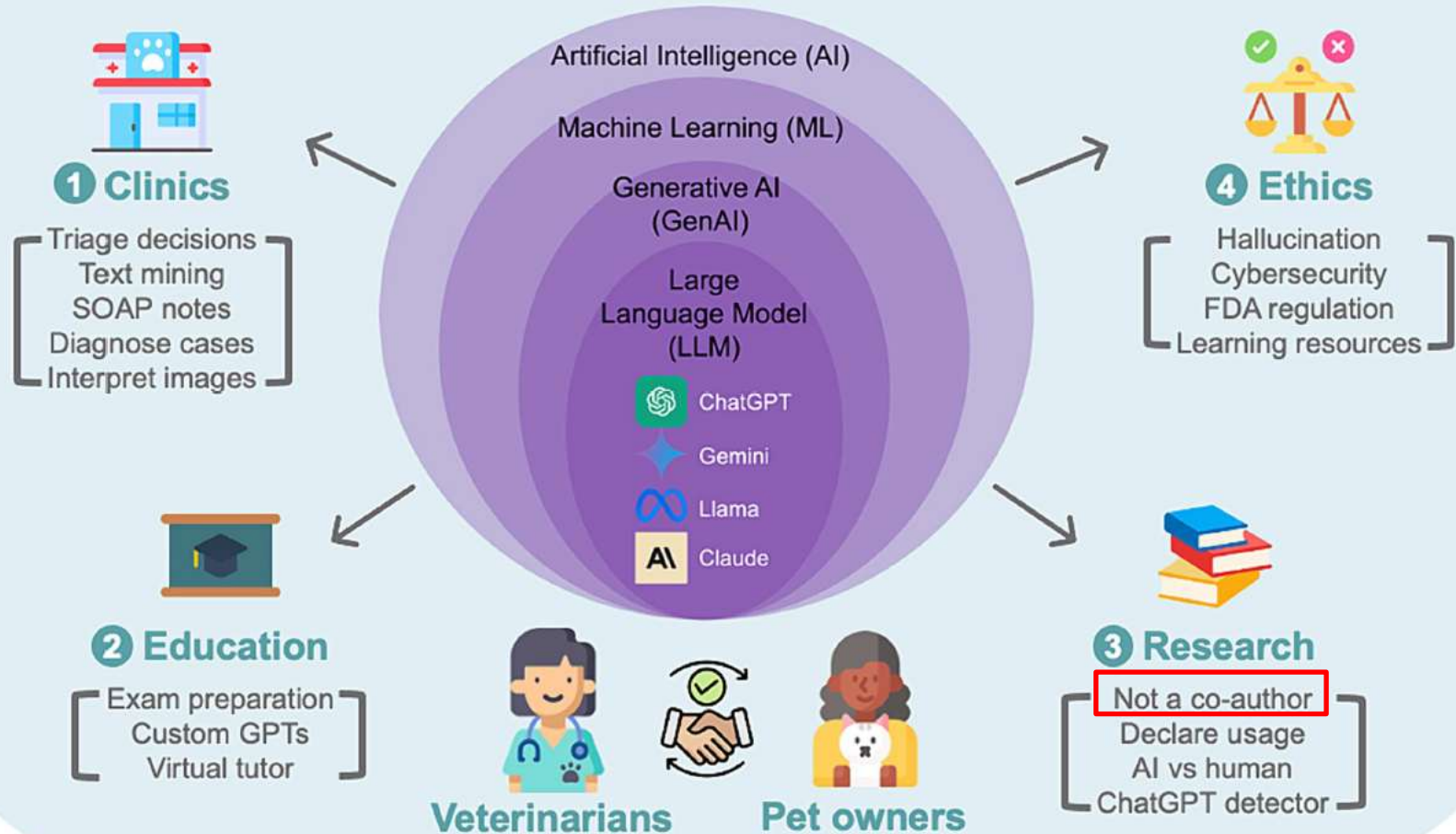


FIGURE 1 Visual abstract of the review.

你提到的這句話「人工智慧於數位毒性病理學之應用」，意思是：

"The application of Artificial Intelligence in Digital Toxicologic Pathology."

簡單來說，就是利用 AI 技術（像是機器學習、深度學習）來分析數位化的毒理病理影像資料，幫助發現毒性反應、診斷病變、甚至預測藥物或化學品對生物體的潛在傷害。這可以大幅提升判讀效率、降低人為誤差，並加速新藥開發或毒性評估的流程。

應用方向總覽

1. 數位影像分析自動化

- 利用 AI 模型（如卷積神經網絡 CNN）辨識病理切片中的異常變化。
- 自動計數細胞、分類細胞異常（如壞死、腫瘤形成等）。

2. 毒性病變偵測與分類

- 快速篩選出可能因藥物或化學品引發的特定組織損傷。
- 建立毒性表徵（toxicological signatures）的資料庫。

3. 病理特徵量化

- 量化如纖維化面積、脂肪變性程度等指標，標準化毒性評估。
- 減少主觀判讀差異，提升數據的一致性與可信度。

4. 預測模型建構

- 基於歷史病理資料，訓練 AI 預測新藥物或物質的潛在毒性。
- 輔助在早期藥物開發階段作出 go/no-go 決策。↓

詢問任何問題



搜尋



推理



深入研究



創作圖像



太好了！來，這裡是針對「人工智慧於數位毒性病理學之應用」的詳細範例，我分成幾個領域來舉例給你：

✦ 1. 病變區域自動標註 (Lesion Annotation)

範例：

使用卷積神經網路 (CNN) 自動在數位病理影像中標記肝臟毒性造成的壞死區域。

應用意義：

- 取代傳統人工標註，節省大量人力。
- 標註結果可以用來訓練後續的診斷或量化模型。

✦ 2. 病變嚴重程度量化 (Severity Scoring)

範例：

AI 模型根據不同病變特徵 (如細胞腫脹、出血、纖維化) 自動給出病變嚴重程度的分數 (如 0-4 級)。

應用意義：

- 標準化不同病理學家之間的評分

詢問任何問題





獨家 / ChatGPT用3年 發現自己變笨了? 權威醫揭人類大腦神經的命運



Discussion



1. **AI provides** an opportunity to merge **large datasets** and **provide insights** that are not possible with the human eye or the human intellect alone
2. **AI is a co-brain** and has the power to transform our ability to see through this complexity and establish **new highly integrated diagnostic signatures**
3. AI will **synergistically improve** a **pathologist's** individual and collective diagnostic efficacy and competency, **not replace them in the future**
4. All revolutions are disruptive. Is it worth it? Once again, **the ball is in our court.**

謝謝您！

